PB86116720

MULTICOMPONENT MODELLING OF FISCHER-TROPSCH SLURRY REACTORS

COUNCIL FOR SCIENTIFIC AND INDUSTRIAL RESEARCH, PRETORIA (SOUTH AFRICA). CHEMICAL ENGINEERING RESEARCH GROUP

AUG 1985

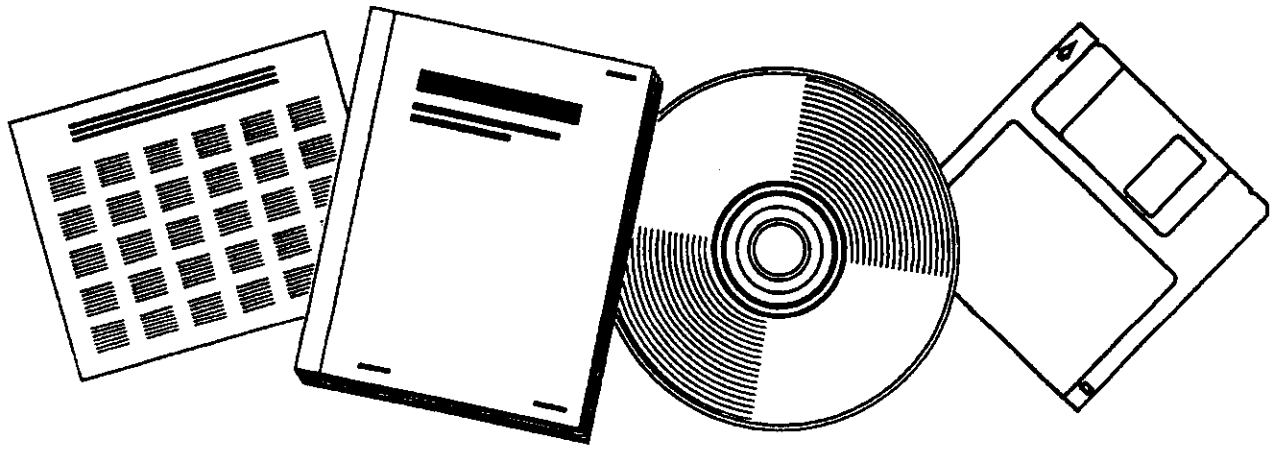

U.S. DEPARTMENT OF COMMERCE
National Technical Information Service

CSIR REPORT CENG 581

MULTICOMPONENT MODELLING OF FISCHER-TROPSCH SLURRY REACTORS

D S VAN VUUREN
M D HEYDENRYCH

CHEMICAL ENGINEERING RESEARCH GROUP – CSIR

COUNCIL for SCIENTIFIC and INDUSTRIAL RESEARCH

Pretoria, South Africa

ISBN 0 7988 3560 5

CSIR REPORT CENG 581

MULTICOMPONENT MODELLING OF FISCHER-TROPSCH SLURRY REACTORS

D S VAN VUUREN
M D HEYDENRYCH

ISBN 0 7988 3560 5

1.a

CSIR REPORT CENG 581

MULTICOMPONENT MODELLING OF FISCHER-TROPSCH SLURRY REACTORS

D S VAN VUUREN
M D HEYDENRYCH

August 1985

Published by the Council for Scientific and Industrial Research
and printed in the Republic of South Africa
by the Graphic Arts Division of the CSIR, Pretoria.

GAcsir 68H4555*8508

CHEMICAL ENGINEERING RESEARCH GROUP
COUNCIL for SCIENTIFIC and INDUSTRIAL RESEARCH

CSIR REPORT CENG 581

MULTICOMPONENT MODELLING OF FISCHER-TROPSCH SLURRY REACTORS

D S VAN VUUREN
M D HEYDENRYCH

CERG - CSIR
P O BOX 395
PRETORIA
0001 RSA

August 1985

SYNOPSIS

In the multicomponent model developed for a Fischer-Tropsch slurry reactor, the water-gas shift reaction is assumed to be in equilibrium. This is supported by literature data on iron-based catalysts above 523 K and synthesis gas conversion above ~ 50 %. A Schulz-Flory product distribution is used.

Investigation of the effects of back-mixing and interphase mass transfer using the model shows that, although the mass transfer rates in full-scale reactors are fast compared with reaction rates, the ratio of the mass transfer rates of reactants and products is important in determining gas velocity and gas hold-up and hence reactor performance.

KEYWORDS: Fischer-Tropsch, slurry reactor, water-gas shift, modelling, mass transfer.

File no: 660-50-2

WNNR-VERSLAG CENG 581

MULTIKOMPONENTMODELLERING VAN FISCHER-TROPSCH FLODDERREAKTORS

D S VAN VUUREN
M D HEYDENRYCH

Augustus 1985

SINOPSIS

In die ontwikkelde multikomponentmodel vir 'n Fischer-Tropsch flodderreaktor word aangeneem dat die watergasreaksie in ewewig is. Die aanname word deur die literatuur oor ysterkatalisators bo 523 K en met 'n sintesegasomsetting bo ~ 50 % bevestig. Vir die produksamestelling word 'n Schulz-Flory verdeling gebruik.

'n Ondersoek van terugmenging en massa-oordrag tussen gas en vloeistof, met gebruikmaking van die model, het gewys dat, hoewel die massa-oordrag in volskaalse reaktors vinnig is in vergelyking met die reaksiesnelheid, die verhouding tussen die massa-oordragstempo's van reaktante en produkte belangrik is, omdat dit die gassnelheid en die gasfraksie en daardeur ook die reaktoreffektiwiteit beïnvloed.

CONTENTS

List of Tables

List of Figures

1. INTRODUCTION

Bubble column slurry reactors are an alternative to the fixed-bed or entrained-bed reactors used in the industrial-scale application of Fischer-Tropsch (F-T) synthesis. In recent reviews[1,2] the main merits of slurry reactors for this purpose were pointed out to be:

- excellent temperature control (heat transfer from a liquid)
- simple mechanical construction
- ability to accept a synthesis gas with a low H_2:CO ratio
- flexible product spectra.

The major disadvantage is lower space-time yields for the same catalyst. However, the potential for superior heat removal makes it possible to use catalysts of high activity compared with those currently used in industrial practice.

In order to understand the interrelation between the physical and chemical processes occurring in slurry reactors and to design and optimize full-scale reactors, a realistic model is required. Calderbank et al.[3] assumed that both the gas and liquid phases are in plug flow, that the liquid flow rate is negligible, and that the reaction rate is first order with respect to the hydrogen concentration. They measured the fluid physical properties separately from the reaction experiments and concluded that both the intrinsic reaction rate and the hydrogen gas-liquid interfacial mass transfer rate are important in determining reactor performance.

Satterfield and Huff[4] derived a model assuming the liquid phase to be perfectly mixed and the gas phase in plug flow. The synthesis gas consumption rate (H_2 plus CO) was assumed to be first order with respect to hydrogen. They analysed data given by Schlesinger et al.[5] and concluded that the hydrogen gas-liquid interfacial mass transfer becomes important at elevated temperatures.

Deckwer et al.[6] analysed the same data using a plug flow model for both gas and liquid phases. They refined the model used by Calderbank et al.[3] as follows: the decrease in gas velocity caused by conversion was accounted for by means of a constant contraction factor, and the consumption ratio of H_2:CO was assumed to be constant throughout the reactor. In contrast to previous workers, they concluded that the hydrogen gas-liquid interfacial mass transfer is negligible in F-T slurry reactors. This was the result of different assumptions about the gas-liquid interfacial area. In a later paper, Quicker and Deckwer[7] presented supporting experimental data.

Bukur[8] and Van Vuuren[9] used the refinements introduced by Deckwer (constant gas contraction and constant H_2:CO consumption ratio) but assumed the gas to be in plug flow and the liquid to be perfectly mixed.

In the meantime Deckwer et al.[10] had derived and used an axial dispersion single-component model to estimate the performance of large-scale F-T slurry reactors. Non-isothermal conditions, intraparticle mass transfer, liquid-solid mass transfer and non-uniform catalyst concentration profiles were incorporated, together with a constant gas contraction factor and H_2:CO consumption ratio. Whereas the models discussed previously yielded algebraic solutions, this model required numerical methods. The analysis indicated that the liquid-solid mass transfer resistance and the catalyst settling rate need not be taken into account.

Stern et al.[11] were the first to use a multicomponent model to analyse mass transfer effects in F-T slurry reactors. They assumed the gas phase to be in plug flow and the liquid phase to be perfectly mixed. The gas velocity change is accounted for by considering the gas-liquid interphase mass transfer of all the reactants and products. They applied their model to four-component reactions, such as the methanation reaction, and concluded that, although the hydrogen mass transfer resistance may be negligible, the ratio of H_2:CO mass transfer rates can cause a high H_2:CO concentration ratio in the liquid phase. In turn, this may influence the average molecular mass of the product formed and the olefin to paraffin ratio in the product.

The ability of slurry reactors to process synthesis gas of low H_2:CO ratios was explained by Satterfield and Huff[12] in terms of the large degree of back-mixing in slurry reactors, the water-gas shift activity of F-T catalysts and the high synthesis gas conversion. This effect, and also the stoichiometry of the F-T reaction and the dependence of the intrinsic reaction rate on the concentrations of H_2O and CO, have not yet been incorporated into advanced slurry reactor models.

The purpose of the present study is to test the simplifying assumptions made by previous workers by means of a suitable model. Effects such as variation of the gas contraction factor and the H_2:CO usage ratio are investigated. The two limiting cases for the liquid phase, perfect mixing and no mixing, are considered. Finite rates of mass transfer are included in the two models: the gas plug flow, perfectly mixed liquid phase model (PMF model), and the gas plug flow, non-mixed liquid phase model (PPF model).

The limit of no mass transfer resistance is derived for the PMF model in the form of an algebraic equation which allows rapid estimation of the reactor performance without having to resort to simplified single-component models. An algebraic equation is also derived for calculating the overall H_2:CO usage ratio.

2. MODELS

In the models derived here the following assumptions have been made:

- the gas phase is in plug flow;
- the products are mainly alkanes;
- the products have a Schulz-Flory (S-F) distribution; and
- the catalyst has sufficient water-gas shift activity for this reaction to be in equilibrium throughout the reactor.

2.1 Gas plug flow; perfectly mixed liquid phase (PMF model)

This model is an extension of the model derived by Stern et al.[11]. In the numerical examples four inorganic reacting compounds, H_2, CO, H_2O and CO_2, and ten alkane products up to decane are taken into account. However, the model does not place a restriction on the number of alkanes that can be used.

The gas phase mass balance equation for each component, written for a differential reactor element, is

$$-\frac{d(U_G C_{G,i})}{dz} = k_{L,i}a\left(\frac{C_{G,i}}{m_i} - C_{L,i}\right) \qquad (1)$$

The overall mass balance for the gas phase is

$$-C_G\frac{dU_G}{dz} = \Sigma k_{L,i}a\left(\frac{C_{G,i}}{m_i} - C_{L,i}\right) \qquad (2)$$

The boundary conditions of Equations (1) and (2) at $z = 0$ are:

$$U_G = U_G^o \text{ and } C_{G,i} = C_{G,i}^o.$$

When no reactants or products enter the reactor in the liquid phase, the liquid phase mass balance for each component is:

$$-Q_L C_{L,i} + \int_o^V k_{L,i}a\left(\frac{C_{G,i}}{m_i} - C_{L,i}\right)dV = V(1-\varepsilon)wr_i \qquad (3)$$

This can be written as:

$$-Q_L C_{L,i} + Vk_{L,i}a\left(\frac{\bar{C}_{G,i}}{m_i} - C_{L,i}\right) = Vw(1-\epsilon)r_i \qquad (4)$$

where $$\bar{C}_{G,i} = \frac{1}{V}\int_o^V C_{G,i}\,dV \qquad (5)$$

These equations can be written in dimensionless form (Stern et al.[11]) using the following definitions:

$$\theta_{G,i} = \frac{C_{G,i}}{C^o_{G,H_2}}, \qquad \nu = \frac{U_G}{U^o_G},$$

$$\theta_{L,i} = \frac{C_{L,i}m_i}{C^o_{G,H_2}}, \qquad \omega_G = \frac{U^o_G}{L},$$

$$\theta_G = \frac{C_G}{C^o_{G,H_2}}, \qquad \omega_L = \frac{Q_L}{V},$$

$$\zeta = \frac{z}{L} \quad \text{and} \quad N_i = \frac{k_{L,i}aL}{m_i U^o_G}$$

The resulting dimensionless equations are:

$$-\frac{d(\nu\theta_{G,i})}{d\zeta} = N_i(\theta_{G,i} - \theta_{L,i}) \qquad (6)$$

$$-\theta_G\frac{d\nu}{d\zeta} = \Sigma N_i(\theta_{G,i} - \theta_{L,i}) \qquad (7)$$

$$\bar{\theta}_{G,i} = \int_o^1 \theta_{G,i}\,d\zeta \qquad (8)$$

and $$-\frac{\omega_L}{\omega_G}\theta_{L,i} + N_i m_i(\bar{\theta}_{G,i} - \theta_{L,i}) = \frac{m_i w(1-\epsilon)r_i}{\omega_G C^o_{G,H_2}} \qquad (9)$$

The boundary conditions at $\zeta = 0$ are:

$$\theta_{G,i} = \frac{C^o_{G,i}}{C^o_{G,H_2}}$$

and $\nu = 1$

To solve Equations (6) to (9) the reaction rate and the stoichiometry of the F-T reaction must be known. Satterfield and Huff[13] measured the reaction rate of the F-T reaction over an iron catalyst in a well-stirred slurry reactor and recommended

$$r_{H_2+CO} = \frac{k_{FT}\, b\, p_{CO} p^2_{H_2}}{p_{H_2O} + b\, p_{CO}\, p_{H_2}} \tag{10}$$

In terms of the dimensionless liquid-phase reactant concentrations, this becomes:

$$r_{H_2+CO} = \frac{k_{FT}\, b\, \theta_{L,CO}\, \theta^2_{L,H_2} (C^o_{G,H_2} RT)^2}{\theta_{L,H_2O} + b\, \theta_{L,CO}\, \theta_{L,H_2} (C^o_{G,H_2} RT)} \tag{11}$$

Equation (11) gives the rate of consumption of synthesis gas, but to solve Equations (6) to (9) the individual consumption rates for H_2 and CO and the individual rates of formation of H_2O and CO_2 are required. These rates also depend on the rate of the water-gas shift reaction, but for iron-based catalysts this reaction may be assumed to be in equilibrium[12,14]. Then

$$\frac{\left(m_{CO_2} C_{L,CO_2} RT\right)\left(m_{H_2} C_{L,H_2} RT\right)}{\left(m_{CO} C_{L,CO} RT\right)\left(m_{H_2O} C_{L,H_2O} RT\right)} = K_w \tag{12}$$

The validity of the assumption will be examined later.

In terms of the dimensionless liquid concentrations,

$$K_w = \frac{\theta_{L,CO_2}\,\theta_{L,H_2}}{\theta_{L,CO}\,\theta_{L,H_2O}} \tag{13}$$

The average stoichiometry of the synthesis reaction (without the water-gas shift reaction) when only alkanes are formed, with a S-F distribution, is[15]:

$$(3 - \alpha)\,H_2 + CO \rightarrow (1 - \alpha)\,C_{1/(1-\alpha)}H_{(4-2\alpha)/(1-\alpha)} + H_2O \tag{14}$$

The stoichiometry of the water-gas shift reaction is:

$$CO + H_2O \leftrightarrows CO_2 + H_2 \tag{15}$$

If n_1 is the rate of consumption of CO via the synthesis reaction and n_2 the rate of consumption of CO via the water-gas shift reaction, the reaction rates of the various inorganic components are:

$$r_{H_2} = (3 - \alpha)n_1 - n_2 \tag{16a}$$

$$r_{CO} = n_1 + n_2 \tag{16b}$$

$$r_{H_2O} = -n_1 + n_2 \tag{16c}$$

and

$$r_{CO_2} = -n_2 \tag{16d}$$

Therefore

$$r_{H_2 + CO} = r_{H_2} + r_{CO} = (4 - \alpha)n_1 \tag{17}$$

and from Equation (9)

$$r_{CO_2} = \frac{\omega_G\, C^o_{G,H_2}}{m_{CO_2}\, w(1 - \varepsilon)}\left(N_{CO_2}\, m_{CO_2}\, (\bar{\theta}_{G,CO_2} - \theta_{L,CO_2}) - \frac{\omega_L}{\omega_G}\,\theta_{L,CO_2}\right) \tag{18}$$

Substituting Equations (16a) to (16d) and Equation (17) into Equation (9) gives:

$$\frac{-\omega_L}{\omega_G}\,\theta_{L,H_2} + N_{H_2}\, m_{H_2}\, (\bar{\theta}_{G,H_2} - \theta_{L,H_2})$$

$$= \frac{m_{H_2} w(1-\varepsilon)}{\omega_G C^0_{G,H_2}} \left(\frac{3-\alpha}{4-\alpha} r_{H_2+CO} + r_{CO_2} \right) \qquad (19)$$

$$\frac{-\omega_L}{\omega_G} \theta_{L,CO} + N_{CO} m_{CO} \left(\bar{\theta}_{G,CO} - \theta_{L,CO} \right)$$

$$= \frac{m_{CO} w(1-\varepsilon)}{\omega_G C^0_{G,H_2}} \left(\frac{r_{H_2+CO}}{4-\alpha} - r_{CO_2} \right) \qquad (20)$$

and $$\frac{-\omega_L}{\omega_G} \theta_{L,H_2O} + N_{H_2O} m_{H_2O} \left(\bar{\theta}_{G,H_2O} - \theta_{L,H_2O} \right)$$

$$= \frac{m_{H_2O} w(1-\varepsilon)}{\omega_G C^0_{G,H_2}} \left(\frac{-r_{H_2+CO}}{4-\alpha} - r_{CO_2} \right) \qquad (21)$$

The rate of formation of each hydrocarbon species is:

$$-r_{C_n} = \frac{(1-\alpha)^2 \alpha^{i-1}}{4-\alpha} r_{H_2+CO} \qquad (22)$$

Substitution into Equation (9) gives:

$$\frac{-\omega_L}{\omega_G} \theta_{L,C_n} + N_{C_n} m_{C_n} \left(\bar{\theta}_{G,C_n} - \theta_{L,C_n} \right)$$

$$= \frac{m_{C_n} w(1-\varepsilon)(1-\alpha)^2 \alpha^{n-1} r_{H_2+CO}}{\omega_G C^0_{G,H_2} (\alpha - 4)} \qquad (23)$$

Equations (6-8), (13), (18-21) and (23) must be solved simultaneously to predict the reactor performance.

The fraction of the total number of molecules leaving the reactor that are hydrocarbons with a carbon number greater than n is:

$$E = \sum_{i=n+1}^{\infty} \frac{(1-\alpha)^2 \alpha^{i-1} X_{CO+H_2}}{(4-\alpha) - 2X_{CO+H_2}} = \frac{(1-\alpha)\alpha^n X_{CO+H_2}}{(4-\alpha) - 2X_{CO+H_2}} \quad (24)$$

The maximum error in the gas flow rate caused by neglecting the hydrocarbons with a carbon number greater than n occurs at total conversion of the synthesis gas:

$$E = \frac{(1-\alpha)\alpha^n}{(2-\alpha)} \quad (25)$$

The chain-growth probability where the error is maximized is:

$$\alpha_m = \frac{(3n+1) - \sqrt{(3n+1)^2 - 8n^2}}{2n} \quad (26)$$

At α_m neglecting hydrocarbons heavier than decane causes a maximum error of 3,2 % at total conversion of the synthesis gas. The error drops to 2,2 % at 90 % gas conversion and optimum chain-growth probability for production of the diesel fraction (α = 0,873). This error is well below that expected from the assumptions made and from the approximations used to calculate the reactor parameters. However, the model allows the use of higher values of n, and the error can thus be reduced.

2.2 Gas plug flow; no mixing in the liquid phase (PPF model)

For these conditions the differential gas-phase mass balance is the same as in the PMF model. The equations can be reduced to

$$\frac{-d\theta_{G,i}}{d\zeta} = \frac{1}{\nu} N_i\left(\theta_{G,i} - \theta_{L,i}\right) - \frac{\theta_{G,i}}{\theta_G \nu} \sum_{i=1}^{\infty} N_i\left(\theta_{G,i} - \theta_{L,i}\right) \quad (27)$$

Because the liquid phase is not mixed and because its nett flow rate is assumed to be negligible:

$$N_i\left(\theta_{G,i} - \theta_{L,i}\right) = \frac{w(1-\varepsilon)}{\omega_G C^o_{G,H_2}} r_i \quad (28)$$

From the Schulz-Flory stoichiometry it follows that:

$$\sum_{i=1}^{\infty} N_i\left(\theta_{G,i} - \theta_{L,i}\right) = \sum_{i=1}^{\infty} \frac{w(1-\varepsilon)}{\omega_G C^o_{G,H_2}} r_i = \frac{w(1-\varepsilon)}{\omega_G C^o_{G,H_2}} \frac{2}{4-\alpha} r_{H_2+CO} \tag{29}$$

Therefore Equation (27) is equivalent to

$$\frac{-d\theta_{G,i}}{d\zeta} = \frac{1}{\nu} N_i\left(\theta_{G,i} - \theta_{L,i}\right) + \frac{2w(1-\varepsilon)\,\theta_{G,i}\, r_{H_2+CO}}{(4-\alpha)\,\omega_G C^o_{G,H_2}\,\theta_G \nu} \tag{30}$$

The gradient of the dimensionless gas velocity is

$$\frac{d\nu}{d\zeta} = -\frac{2w(1-\varepsilon)\, r_{H_2+CO}}{(4-\alpha)\,\omega_G \theta_G C^o_{G,H_2}} \tag{31}$$

In order to solve Equations (30) and (31), one needs to consider only the four inorganic components (H_2, CO, CO_2 and H_2O) since the effect of the organic products on the changes in the total gas flow rate is taken into account by Equation (31). Note that the concentrations of the hydrocarbon products do not affect the intrinsic rate of conversion of the synthesis gas.

Equation (30) with the boundary condition

$$\theta_{G,i} = C^o_{G,i} / C^o_{G,H_2} \quad \text{at } \zeta = 0$$

must be solved while the following equations are satisfied:

$$N_{H_2}\left(\theta_{G,H_2} - \theta_{L,H_2}\right) - \frac{w(1-\varepsilon)}{\omega_G C^o_{G,H_2}}\left(\frac{3-\alpha}{4-\alpha} r_{H_2+CO} + r_{CO_2}\right) = 0 \tag{32a}$$

$$N_{CO}\left(\theta_{G,CO} - \theta_{L,CO}\right) - \frac{w(1-\varepsilon)}{\omega_G C^o_{G,H_2}}\left(\frac{1}{4-\alpha} r_{H_2+CO} - r_{CO_2}\right) = 0 \tag{32b}$$

$$N_{H_2O}\left(\theta_{G,H_2O} - \theta_{L,H_2O}\right) - \frac{w(1-\varepsilon)}{\omega_G C^o_{G,H}}\left(\frac{-1}{4-\alpha} r_{H_2+CO} - r_{CO_2}\right) = 0 \tag{32c}$$

and the water-gas shift equation

$$\frac{\theta_{L,CO_2}\,\theta_{L,H_2}}{\theta_{L,CO}\,\theta_{L,H_2O}} - K_W = 0 \qquad (32d)$$

2.3 No mass transfer resistance in PMF model

The additional assumption is made that the reactants and products leaving the reactor in the liquid phase are negligible compared with those leaving in the gas phase. If the gas-liquid mass transfer resistance is assumed to be negligible, a mixed liquid phase now implies that the gas phase concentrations are constant.

If for each mole of CO and H_2 fed to the reactor t_1 moles of CO are converted via the F-T reaction and t_2 moles via the water-gas shift reaction, it follows that

$$U_G = U_G^o\left(1 - \frac{2}{4-\alpha}\,X_{CO+H_2}\right) \qquad (33)$$

and

$$t_1 = \frac{X_{CO+H_2}}{4-\alpha} \qquad (34)$$

Mole fractions of H_2, CO, H_2O and CO_2 are:

$$y_{H_2} = \frac{[1/(1+1)] - \left((3-\alpha)X_{CO+H_2}/(4-\alpha)\right) + t_2}{1 - [2/(4-\alpha)]X_{CO+H_2}} \qquad (35a)$$

$$y_{CO} = \frac{[1/(1+1)] - X_{CO+H_2}/(4-\alpha) - t_2}{1 - [2/(4-\alpha)]X_{CO+H_2}} \qquad (35b)$$

$$y_{H_2O} = \frac{X_{CO+H_2}/(4-\alpha) - t_2}{1 - [2/(4-\alpha)]X_{CO+H_2}} \qquad (35c)$$

$$y_{CO_2} = \frac{t_2}{1 - [2/(4-\alpha)]X_{CO+H_2}} \qquad (35d)$$

and

$$y_{C_n} = \frac{(1-\alpha)^2\,\alpha^{n-1}\,X_{CO+H_2}/(4-\alpha)}{1 - [2/(4-\alpha)]X_{CO+H_2}} \qquad (35e)$$

Assuming the water-gas shift reaction to be in equilibrium

$$t_2 = \frac{B - \sqrt{B^2 - 4AC}}{2A} \tag{36a}$$

where $$A = K_w - 1 \tag{36b}$$

$$B = \frac{K_w + 1}{1 + 1} - \frac{3 - \alpha}{4 - \alpha} X_{CO+H_2} \tag{36c}$$

and $$C = \frac{K_w}{4 - \alpha}\left(\frac{1}{1 + 1} - \frac{X_{CO+H_2}}{4 - \alpha}\right) X_{CO+H_2} \tag{36d}$$

It also follows that the usage ratio (moles of H_2 converted per mole of CO converted) is

$$U = \frac{2A(3 - \alpha)X_{CO+H_2} - (B - \sqrt{B^2 - 4AC})(4 - \alpha)}{2AX_{CO+H_2} + (B - \sqrt{B^2 - 4AC})(4 - \alpha)} \tag{37}$$

Since the gas and liquid phases are in equilibrium, the dimensionless liquid-phase concentrations are

$$\theta_{L,i} = (1 + 1)y_i/1 \tag{38}$$

A mass balance over the reactor gives

$$X_{CO+H_2} = \left[\frac{w(1 - \varepsilon)}{\omega_G \theta_G C^o_{G,H_2}}\right]\left[\frac{k_{FT} b\theta_{L,CO}\theta^2_{L,H_2}(C^o_{G,H_2}RT)^2}{\theta_{L,H_2O} + b\theta_{L,CO}\theta_{L,H_2}(C^o_{G,H_2}RT)}\right] \tag{39}$$

Equation (39) can be solved iteratively by guessing a value for the total synthesis gas conversion. Equations (36a-36d) then give t_2 and the result is substituted in Equations (35a-35c) to calculate the H_2, CO and H_2O mole fractions in the outlet. The dimensionless liquid phase concentrations follow from Equation 38. These can now be substituted in Equation (39) for comparison with the previous guess of X_{CO+H_2}. Once satisfactory convergence has been obtained, the dimensionless CO_2 and hydrocarbon liquid concentrations are calculated from Equations (35d), (35e) and (38).

3. NUMERICAL METHODS

Correlations used for estimating the various parameters are given in the Appendix. Velocity-dependent parameters, for instance the gas hold-up and the bubble diameter, were assumed to be constant at 0,45 and 7×10^{-4} m respectively, except in those examples where the effect of mass transfer rates was considered. In such cases the gas hold-up was estimated from the average gas velocity, as detailed in the Appendix.

The PMF model was solved by first estimating the liquid-phase concentrations using the simpler version, assuming no mass transfer resistance. The gas-phase mass balance equations were then solved using a fourth order Runge-Kutta method. Owing to the stiffness of the differential equations, 400 steps were required to ensure convergence. Average gas phase concentrations were calculated using Equation (8). The rate of CO_2 consumption calculated from Equation (18), the calculated gas phase concentrations and the estimated liquid phase concentrations were then substituted into Equations (13), (19-21) and (23) to calculate errors. These errors were then used to estimate improved liquid phase concentrations using the Newton Raphson technique[16]. Because the mass transfer resistances were found to be relatively unimportant, the initial estimates of the liquid phase concentrations were close to the final values so that satisfactory convergence followed after three to four iterations in most cases.

The PPF model equations were solved by first assuming values for θ_{L,H_2}, $\theta_{L,CO}$, θ_{L,H_2O} and θ_{L,CO_2} in each reactor increment. The CO_2 consumption rate was calculated from Equation (28) and the synthesis gas conversion rate from Equation (11). Substitution of the guessed liquid concentration and the calculated reaction rates into Equations (32a-32d) gave errors from which improved values for the liquid phase concentrations were calculated until satisfactory convergence was obtained. The final values were then substituted into Equations (30) and (31) to solve the system of differential equations by the Runge-Kutta method; 50 reactor increments proved to be sufficient.

4. RESULTS AND DISCUSSION

4.1 Water-gas shift equilibrium

Satterfield and Huff[12] theorized that the water-gas shift reaction proceeds to equilibrium in F-T slurry reactors operating with iron-based catalysts. They presented a few data points to support their argument.

On the other hand, when studying the F-T synthesis rate over iron catalysts in a fixed-bed reactor, Dry et al.[17] found that the water-gas shift reaction is a secondary reaction and that it is not in equilibrium at the reactor outlet. However, the retention times used in fixed-bed reactors are normally much shorter than in slurry reactors. Dry et al.[17] used a retention time of 1 s in their fixed-bed reactor, whereas retention times of more than 80 s were employed in the slurry reactor used in the Rheinpreussen-Koppers demonstration plant (Kolbel and Ralek[1]). Therefore the assumption that the water-gas shift reaction is in equilibrium in slurry reactors might be reasonable. Alternatively, a finite rate must be incorporated into the model for the water-gas shift reaction.

In the following paragraphs Equations (35a), (35b) and (37) are applied to experimental data for F-T slurry reactors presented in the literature. It should be noted that, although the equations were derived for a perfectly mixed reactor where the gas and liquid phases are in equilibrium, they are equally valid for any type of reactor as long as the gas and liquid phases are in equilibrium at the reactor outlet. This condition is normally approached in large-scale reactors.

In Table 1 experimental data for the hydrogen to carbon monoxide usage ratios reported by Farley and Ray[18] are compared with theoretical data. Chain-growth probabilities were calculated from the reported C_5^+ fractions using the formulae for the S-F distribution derived by Caldwell[19]. The reported gas contraction data are also compared with the theoretical contraction predicted by Equation (33). A precipitated iron catalyst promoted by potassium and copper oxides was used. The agreement as regards contraction is excellent, but the theory generally predicts slightly higher usage ratios than have been reported. However, if the water-gas shift did not reach equilibrium, the experimental usage ratios should have been higher than predicted. It is therefore concluded that the water-gas shift reaction was in equilibrium in this case.

The difference between theory and experiment is ascribed to

i. the gas and liquid phases probably not being in true equilibrium,

ii. all the products being regarded in theory as paraffins, whereas the olefins and oxygenates also affect the stoichiometry, and

iii. the estimates of the chain-growth probability being only approximate.

TABLE 1 Usage ratio and gas contraction reported by Farley and Ray[19]

Period	T (K)	X (%)	Alpha[1]	U, exp	U, pred	Y, exp	Y, pred
1	533	59, 1	0, 875	0, 565	0, 579	39, 6	37, 8
3	538	55, 7	0, 849	0, 534	0, 585	36, 2	35, 4
5	548	54, 7	0, 799	0, 565	0, 611	34, 6	34, 2
7	548	52, 7	0, 817	0, 528	0, 602	33, 2	33, 1
9	548	50, 8	0, 741	0, 554	0, 640	31, 7	31, 2
11	548	49, 3	0, 771	0, 530	0, 625	30, 6	30, 5
13	553	45, 1	0, 751	0, 646	0, 635	27, 5	27, 8

1. Alpha calculated from pentane and heavier mass fraction

Table 2 compares the hydrogen to carbon monoxide usage ratios and gas contractions as calculated from the data presented by Schlesinger et al.[20] with those predicted by the theory. Chain-growth probabilities were derived from the reported C_3^+ fractions. Precipitated iron promoted by copper and alkali was used as the catalyst.

TABLE 2 Usage ratio and gas contraction reported by Schlesinger et al.[20]

Time (h)	T (K)	X (%)	Alpha[1] .	U, exp .	U, pred .	Y, exp (%)	Y, pred (%)
110	515	62	0, 846	0, 57	0, 60	43	39
295	528	60	0, 770	0, 60	0, 64	43	37
405	527	45	0, 779	0, 61	0, 63	31	28
570	528	60	0, 792	0, 62	0, 62	41	37
830	534	55	0, 783	0, 63	0, 63	37	34
1000	548	50	0, 771	0, 61	0, 64	33	31

1. Alpha calculated from propane and heavier mass fraction

As in the previous case[18], the theoretical usage ratios are slightly higher than the experimental values, but in this case there is better agreement. The contraction factor data, on the other hand, correspond less well with the theory. Again it can be concluded that for all practical purposes the water-gas shift reaction was close to equilibrium during all the experimental runs, and the differences between the theoretical and measured results are ascribed to the same effects as in the previous study.

In a later paper Schlesinger et al.[5] reported on slurry reactor experiments in which an iron nitride catalyst was used. Considerably more oxygenates were produced and a longer catalyst life was reported. The theoretical and experimental usage ratios (Table 3) show that in all cases the reported usage ratios were higher than the theoretical values. At higher temperatures the discrepancies decreased. Although the reported mass balances were only about 93 % correct, it is concluded that the water-gas shift activity of the iron nitride catalyst is lower than that of the precipitated iron catalysts, so much so that the water-gas shift reaction cannot be taken to be in equilibrium.

TABLE 3 Usage ratio reported by Schlesinger et al.[5]

T (K)	X (%)	Alpha[1]	U, exp	U, pred
493	22, 0	0, 707	0, 96	0, 65
503	29, 0	0, 687	0, 94	0, 66
513	44, 9	0, 678	0, 87	0, 67
523	62, 0	0, 639	0, 83	0, 70
531	71, 4	0, 573	0, 81	0, 74

1. Alpha calculated from propane and heavier mass fraction.

Koppers[21] reported on the operating conditions, the conversion, and the product spectrum of the Rheinpreussen-Koppers demonstration plant, in which alkali-promoted iron catalysts were used. The data relevant to the present discussion are: temperature = 541 K, inlet H_2:CO ratio = 0,667, H_2 plus CO conversion = 89 %, CO conversion = 91 % and C_3^+ mass fraction = 91,7 %. The overall conversion, the CO conversion and the inlet ratio give a calculated H_2:CO usage ratio of U = 0,63. An estimate of the chain-growth probability from the C_3^+ mass fraction gives α = 0,823. The theoretical usage ratio is then, U = 0,61. The theoretical and experimental usage ratios are therefore almost equal and it is concluded that the water-gas shift reaction approached equilibrium.

In a recent investigation by Deckwer et al.[14] of slurry-phase synthesis, using a potassium-promoted precipitated iron catalyst, operating conditions, conversion ratios and usage ratios were reported, but unfortunately product spectra were not. For the purpose of this study it was therefore assumed that the chain-growth probability was 0,85 in all cases (lower values of α give higher predicted than experimental usage ratios at high temperatures). In Figure 1 the data are presented

with the calculated theoretical usage ratio. For temperatures below 240 °C, the theory predicts usage ratios well below the experimental values, whereas above 240 °C the theoretical values tend to match the experimental data. It is therefore concluded that below 240 °C the water-gas shift activity drops significantly, and the reaction cannot be taken to be in equilibrium.

FIGURE 1 Usage ratio measured by Deckwer et al.[14]

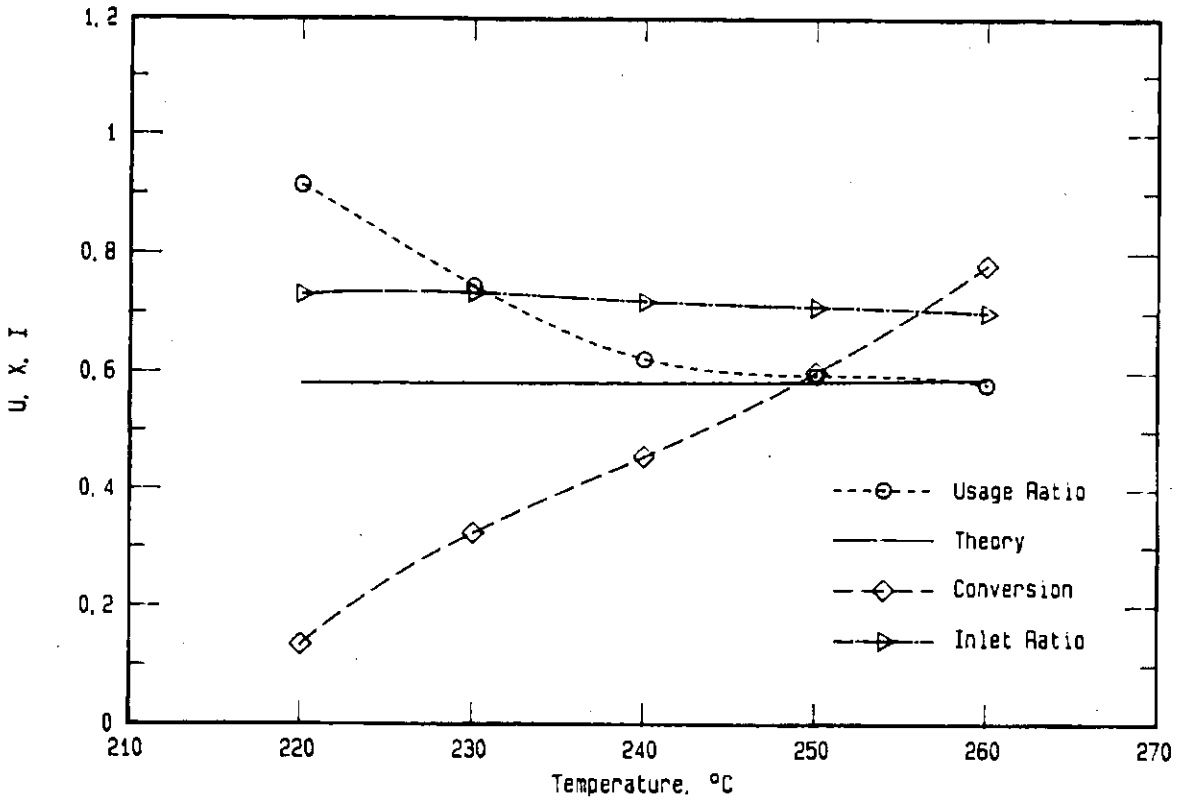

Deckwer et al.[14] also reported on the dependence of the usage ratio on the gas velocity. In Figure 2 their data and the theory are compared. At low velocities the theory predicts the observed usage ratio data satisfactorily, but not at higher velocities. Since the water-gas shift reaction must have a finite rate, it follows that if the retention time of the gas in the reactor is too short the reaction cannot be assumed to be in equilibrium.

FIGURE 2 Usage ratio measured by Deckwer et al.[14]

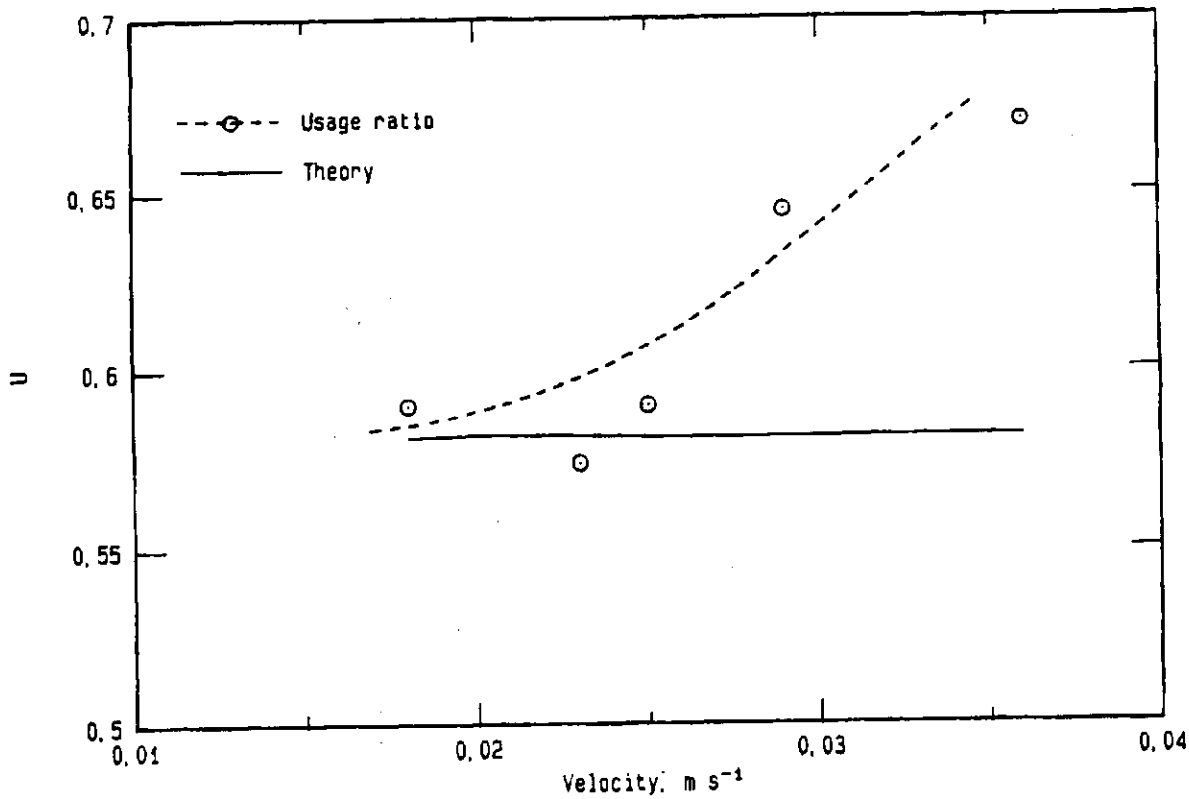

The last study considered here is an investigation by Kuo et al.[22] in which a two-stage F-T product conversion process was investigated. In the first stage synthesis took place in the slurry phase, and in the second phase the product spectrum was altered by using a ZSM-5 catalyst. An iron catalyst promoted by copper and potassium carbonate was used.

In Figure 3 the experimental outlet hydrogen to carbon monoxide ratios reported[22] are compared with those predicted. The reported chain-growth probability of 0,79 for the hydrocarbons of carbon number less than 22 was used in the theoretical calculations. The match between the theory and experimental data is good at conversions below 80 %. Above 80 % for inlet ratios of 0,7, the observed ratios are above the theoretical ratios, meaning that the water-gas shift reaction went past the equilibrium point to the right-hand side of Equation (18). This is clearly impossible since the synthesis reaction is primary to the water-gas shift reaction[17]. This discrepancy is again related to the assumptions of the model, viz. that the gas and liquid phases are in equilibrium at the reactor exit and that all the products are alkanes, and also to experimental error as is evident from the wide scatter in the data. Again it is concluded that the water-gas shift reaction approached equilibrium.

FIGURE 3 Exit H_2:CO ratio measured by Kuo et al.[22]

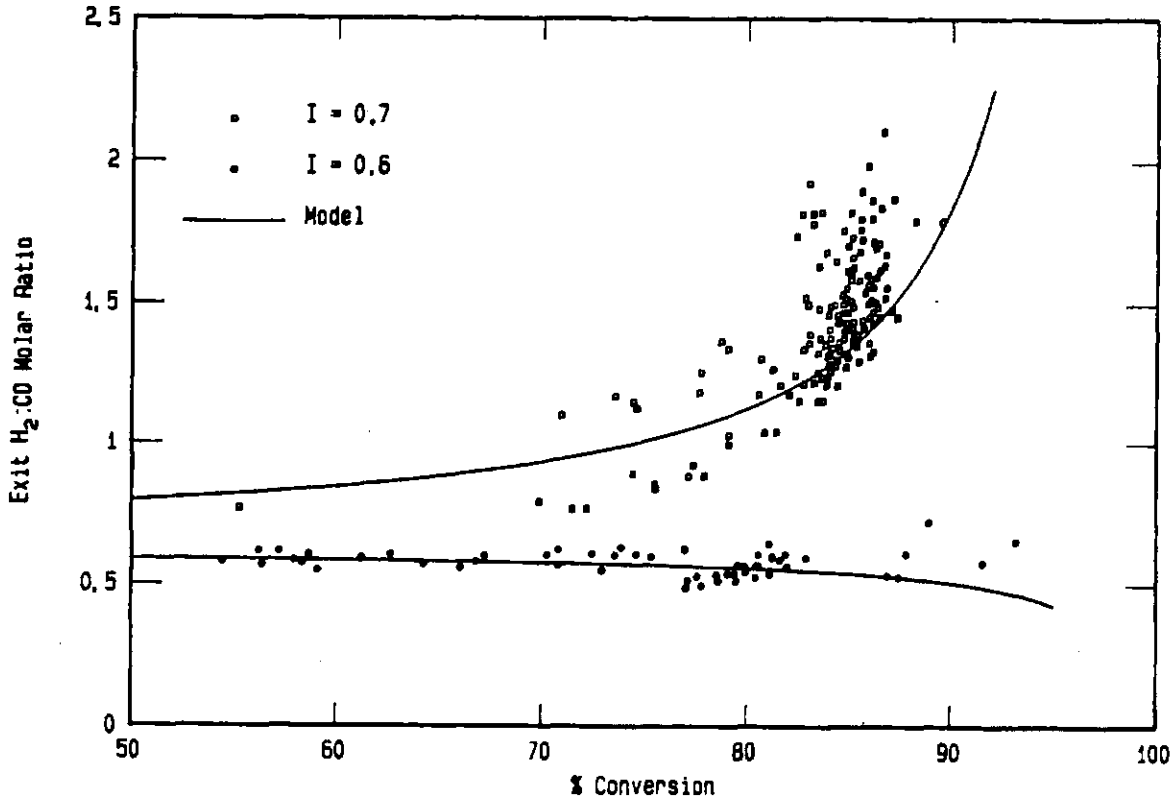

The agreement between experimental data and theory shown in Figure 3 confirms the view of Satterfield and Huff[12] that the ability of slurry reactors to process synthesis gas of low H_2:CO ratio is related to the high water-gas shift activity of the catalyst, high conversion and a large degree of back-mixing.

Synthesis catalysts such as ruthenium, which usually have low water-gas shift activity under synthesis conditions[23,24], must therefore not be used in slurry reactors if it is intended to obtain the full benefit of the lower cost of synthesis gas with a low hydrogen to carbon monoxide ratio. The often quoted advantage of slurry reactors, that they give high single-pass conversions, is not a true advantage, but a prerequisite for using the cheaper synthesis gas, as shown by the above theory; high single-pass conversions decrease recycling costs, but also decrease space-time yields.

4.2 Gas plug flow; perfectly mixed liquid phase (PMF model)

In Figure 4 the H_2, CO, H_2O and CO_2 concentration profiles as predicted by the PMF model for the Rheinpreussen-Koppers slurry reactor[21] are plotted. The catalyst activity was chosen so as to predict the reported conversion approximately. The gas concentrations change rapidly in the initial section of the reactor and then

remain constant through about 80 % of the reactor. The constant value is not equal to the equilibrium value, but it can be seen that about 95 % of the total difference between the inlet concentrations and the equilibrium values is achieved within only about 20 % of the reactor space.

FIGURE 4 H_2, CO, CO_2 and H_2O concentrations predicted by PMF model

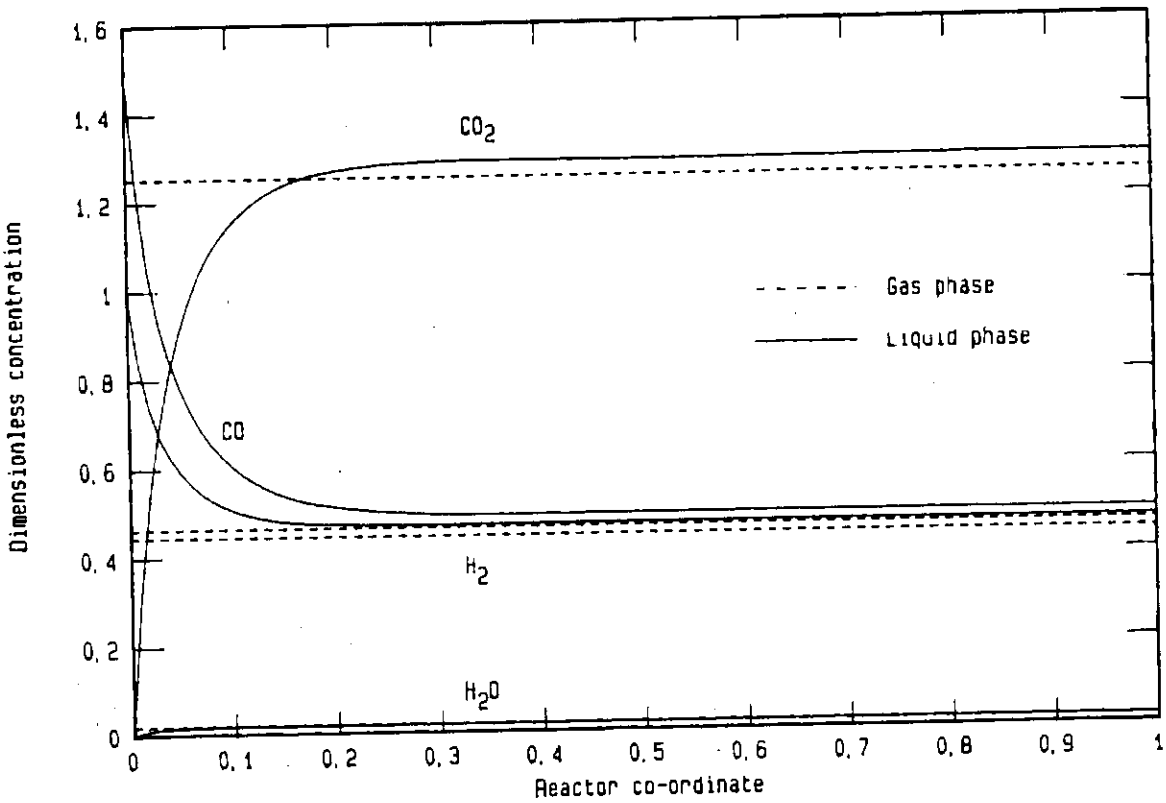

In Figure 5 some of the hydrocarbon concentration profiles are plotted against the reactor co-ordinate. The higher the carbon number, the more rapidly it approaches a constant value close to the equilibrium value. For decane only 2 % of the reactor space is required to reach this constant value. The reason for this phenomenon is that the higher the hydrocarbon number, the lower the solubility coefficient and the higher the Stanton number becomes. Because of this effect, it can be assumed that all the hydrocarbons heavier than decane are in gas-liquid equilibrium throughout the reactor.

FIGURE 5 Hydrocarbon concentrations predicted by PMF model

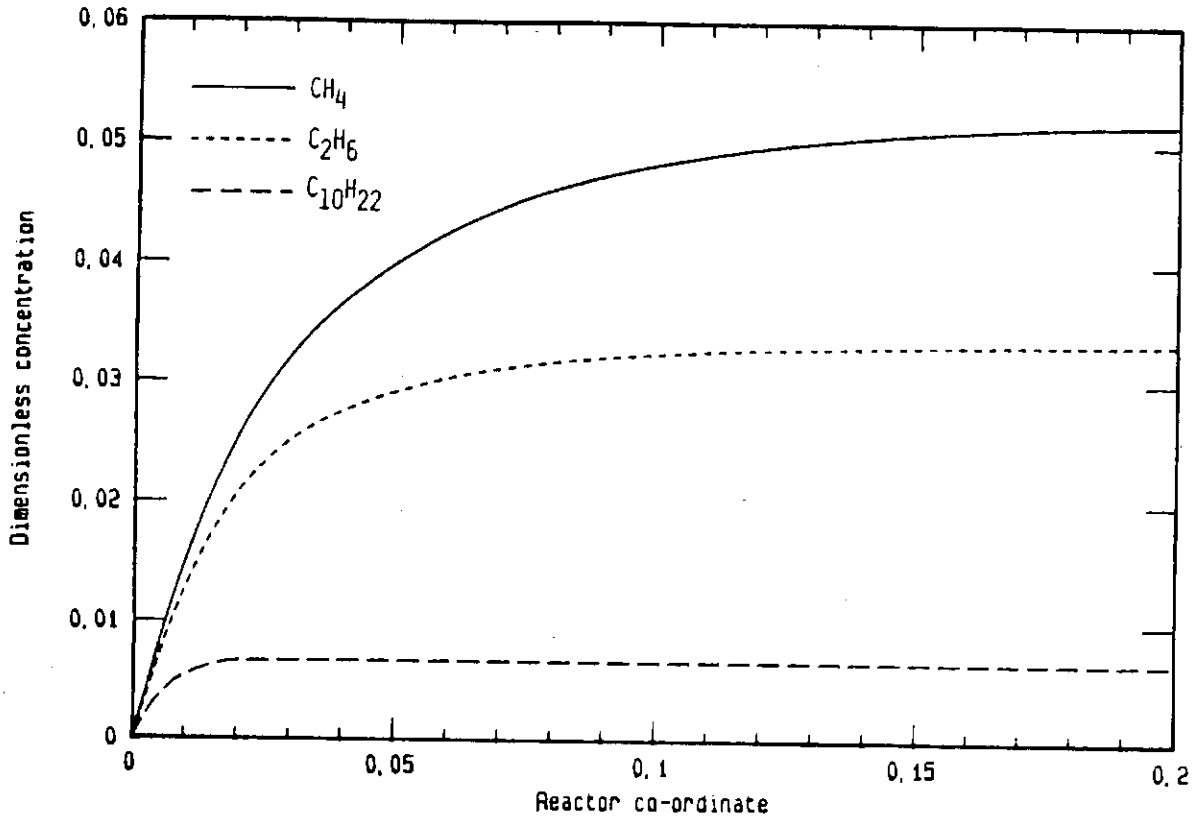

The necessity to use 400 step-sizes in the computer program to solve the system of equations is related to the high Stanton numbers of the hydrocarbon products, which cause the differential gas phase mass balance equations to become stiff. The number of step-sizes can probably be reduced by choosing a varying step length, but this possibility was not explored.

In various reactor models[4,6,9,10] the gas velocity was assumed to be a linear function of the synthesis gas conversion, and the usage ratio was assumed to be constant throughout the reactor. (The conversion was defined as the ratio of the number of moles of synthesis gas crossing the gas-liquid interfacial boundary to the number of moles of synthesis gas entering the reactor, and the usage ratio was defined as the ratio of the rates of interfacial mass transfer of hydrogen to carbon monoxide.) In order to test these assumptions, the superficial gas velocity predicted by the model is compared in Figure 6 with that predicted using a constant contraction factor. The conversion and the usage ratio predicted by the model are also shown. It is clear that the simplifying assumptions of a constant contraction factor, conversion-dependent gas velocity and a constant usage ratio are invalid.

FIGURE 6 V, X and U predicted by PMF model

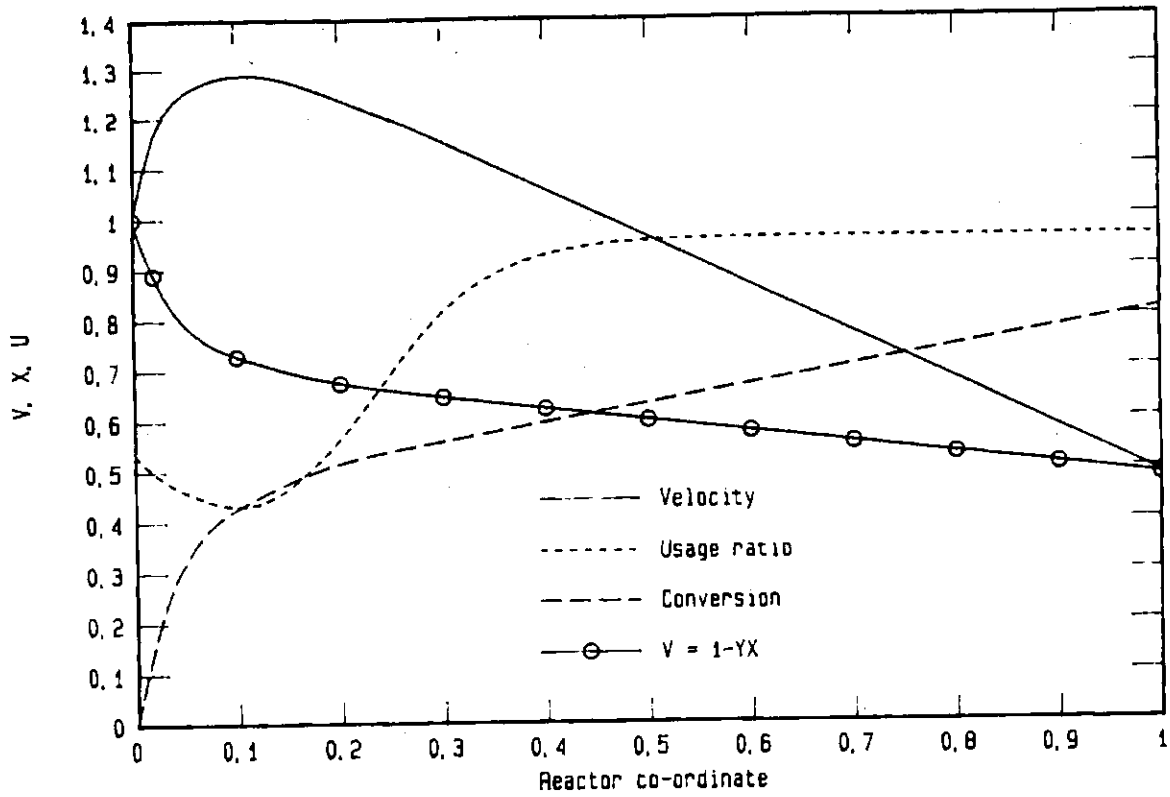

Another interesting phenomenon is the initial increase (~ 30 %) in superficial gas velocity. This effect was unexpected since all the previous models in the literature predicted a convex monotonic decrease in gas velocity with the reactor co-ordinate. Since the gas velocity is the most important parameter affecting the gas hold-up, the slurry hold-up and therefore the reactor space available for the catalyst, this finding is of considerable importance. In Section 4.5 this effect is discussed in detail.

4.3 Gas plug flow; no mixing in the liquid phase (PPF model)

In Figure 7 the gas and liquid phase concentration profiles as predicted by the PPF model are given. The catalyst activity and the operating conditions are the same as those used in Figure 4 in which the Rheinpreussen-Koppers slurry reactor is simulated by the PMF model. Since the difference between the gas and liquid phase concentrations is about 10 % of the gas phase concentration, the mass transfer resistance is about 10 % of the total resistance. In Figure 8, the dimensionless velocity, the conversion and the usage ratio profiles are plotted. In the PPF model

the velocity is a linear function of conversion and follows Equation (33). The usage ratio is also remarkably constant up to a reactor co-ordinate of 0,6 at which point the overall conversion is about 80 %. It appears therefore that the PPF model of Deckwer et al.[6] in which the usage ratio is assumed to be constant and the gas velocity is a linear function of conversion, can indeed be used to evaluate reactors with high length-to-diameter ratios operating at moderate conversions (less than 80 %).

FIGURE 7 H_2, CO, CO_2 and H_2O concentrations predicted by PPF model

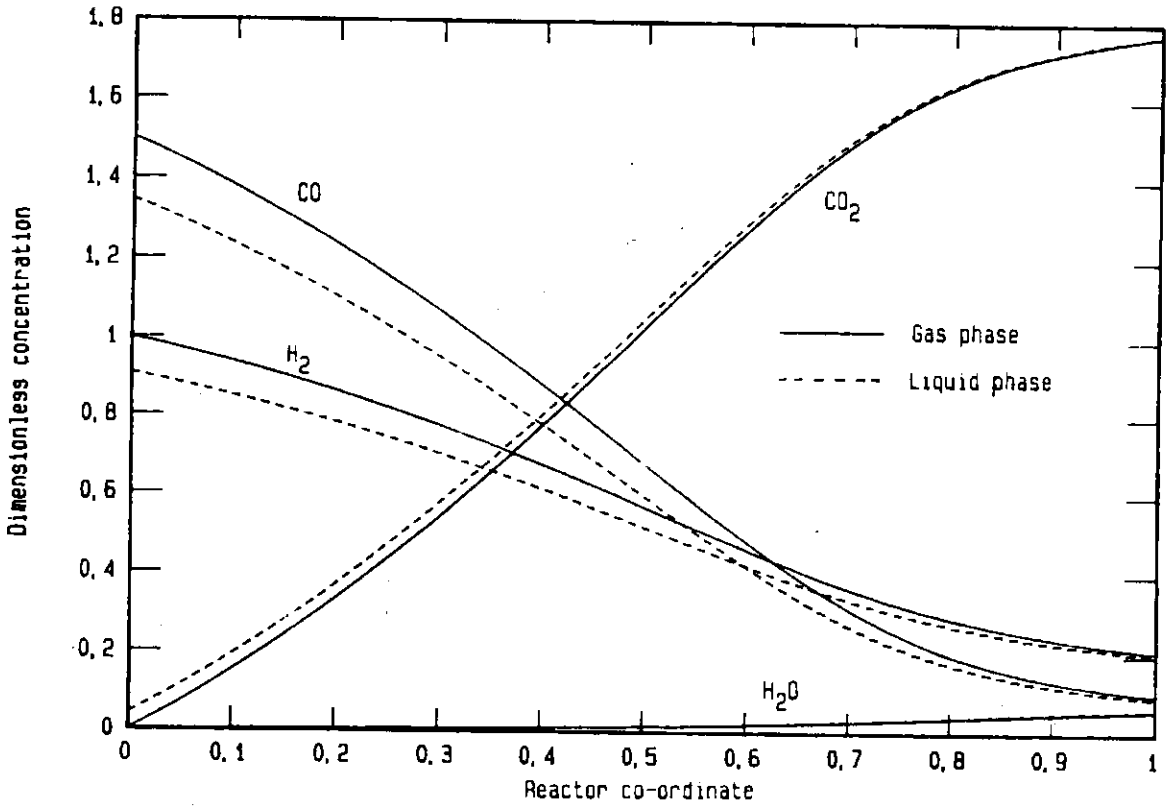

FIGURE 8 V, X and U predicted by PPF model

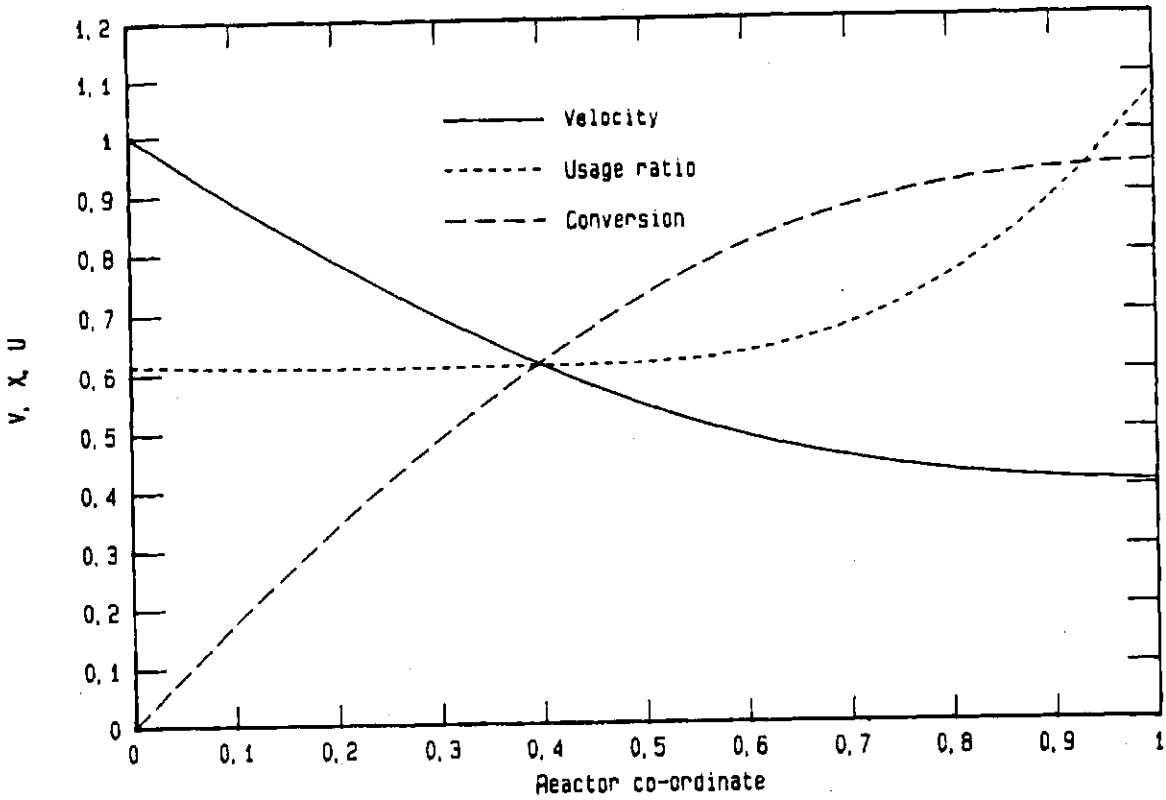

4.4 Comparison of PMF and PPF models

In Figures 9 and 10 the effect of catalyst activity and reactor length on overall conversion is illustrated using the two reactor models. As can be expected from elementary reactor technology principles, there is not much difference between the two models at conversions below 40 %, but the effect of liquid mixing increases dramatically at higher conversions. To obtain high conversions in large-scale slurry reactors it would clearly be advantageous to decrease the degree of mixing in these reactors by baffling or stageing. Some back-mixing must, however, be retained to allow the use of synthesis gas with low hydrogen to carbon monoxide ratios (see discussion on the water-gas shift equilibrium).

FIGURE 9 Effect of catalyst activity

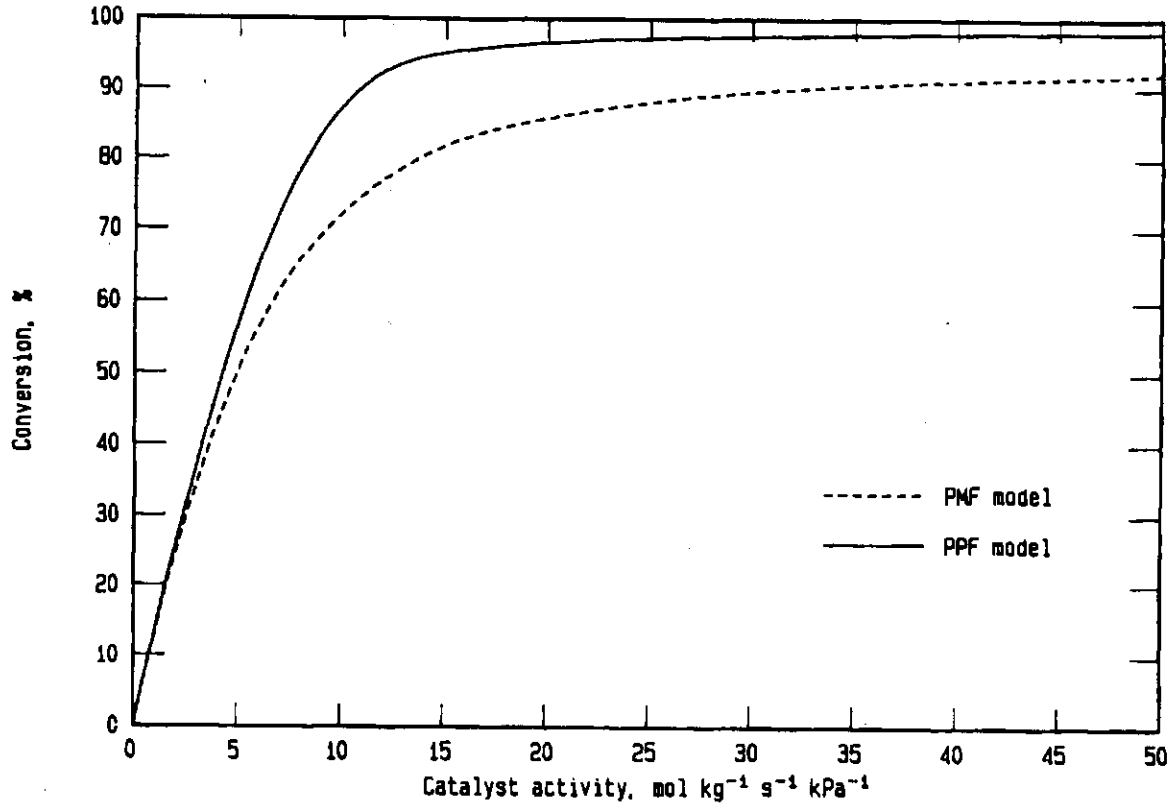

FIGURE 10 Effect of reactor length

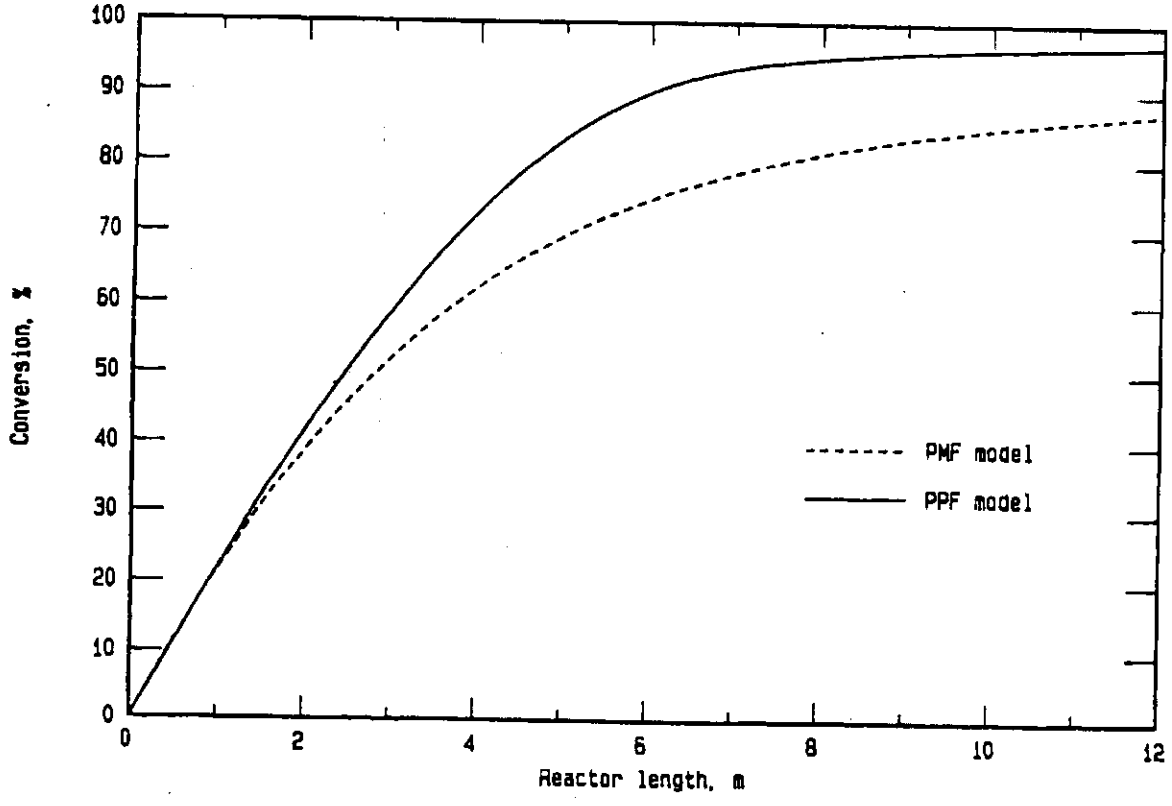

4.5 The influence of mass transfer

The effect of mass transfer on overall conversion at constant gas hold-up in large reactors is illustrated in Figure 11. The catalyst activity was again chosen so that the overall conversion corresponds approximately to that reported for the Rheinpreussen-Koppers demonstration plant[21] and the interfacial area was varied by changing the bubble size. At a bubble diameter of $1,5 \times 10^{-3}$m, which is more than twice that reported by Quicker and Deckwer[7], the conversion is only about 2,6 % lower than in the case of infinite mass transfer rates. This makes the reactor model with no mass transfer resistance and perfect mixing a useful tool for the rapid estimation of reactor performance, without the need to make unrealistic assumptions about the usage ratio or the gas velocity contraction factor, but retaining the complexity of the synthesis reaction rate expression that is required at high conversions.

FIGURE 11 Effect of mass transfer on conversion

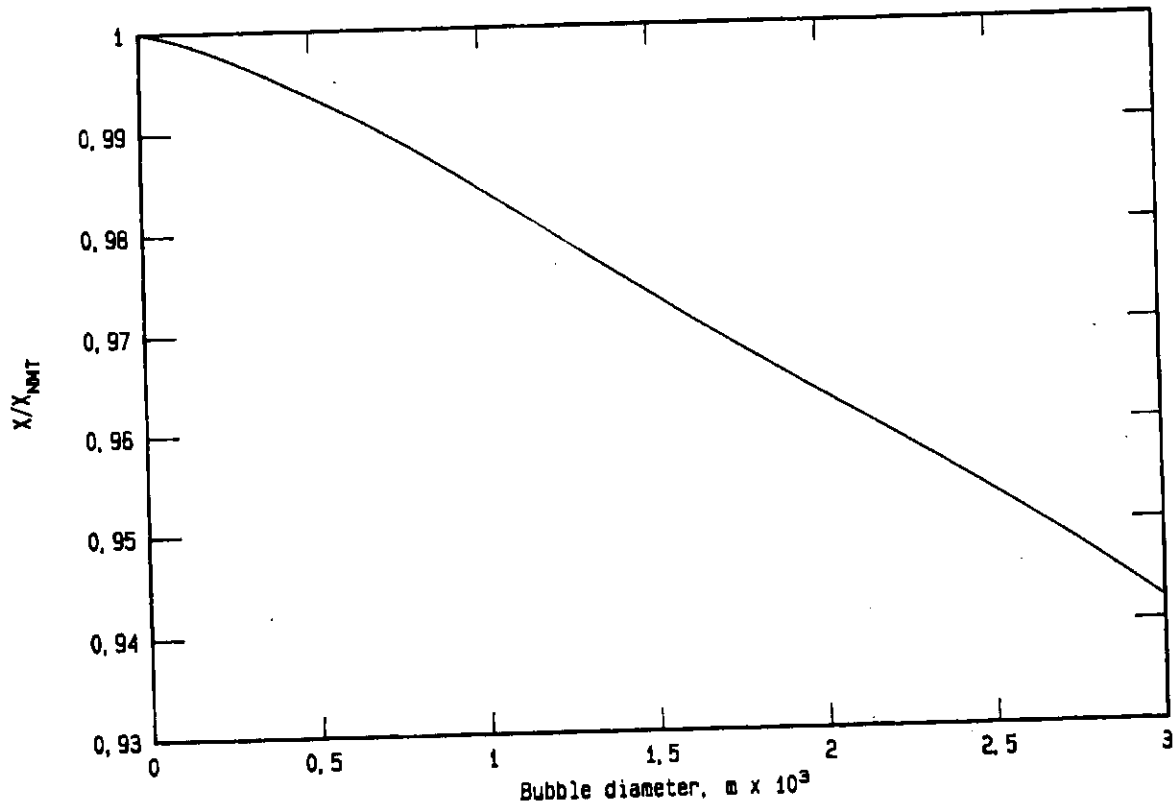

However, when the influence of the velocity profile on the gas hold-up is considered, the effect of the ratios of the mass transfer rates of the reactants and products becomes important. Because of the high degree of back-mixing in slurry reactors, products are transported back to the inlet via the liquid phase. Here their rate of transfer to the gas phase can be higher than the rate of transfer of the reactants to the liquid phase, so that an initial increase in gas velocity may result. Higher up in the reactor, excess products in the gas phase are absorbed into the liquid phase.

In Figure 12 the effect of the CO_2 diffusivity on the velocity profile at constant gas hold-up is illustrated by changing its magnitude arbitrarily relative to the value estimated in the Appendix. Either an initial increase or an initial decrease in gas velocity occurs, depending on the ratios of the mass transfer rates of the reactants and products. In spite of this large effect on the velocity profile, the overall conversion remains almost unaffected since the gas hold-up is kept constant.

FIGURE 12 Effect of CO_2 diffusivity

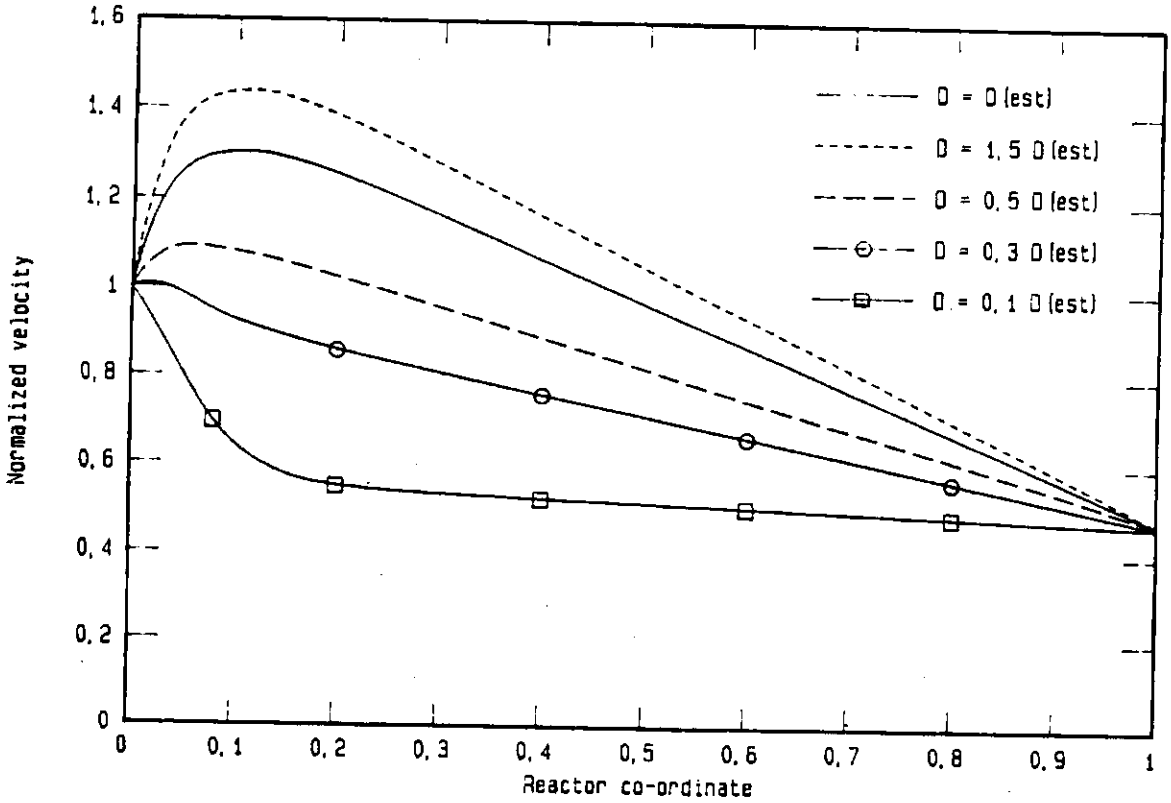

In order to quantify the effect of the changing velocity profile on conversion, the gas hold-up was changed from its constant value of 0,45 to the value predicted by the correlation of Deckwer et al.[25] using the average superficial gas velocity. The results (see Table 4) demonstrate that, although the mass transfer resistance is small compared with the kinetic resistance, the ratios of the mass transfer rates of reactants and products are important for the correct prediction of overall reactor performance.

TABLE 4 Effect of CO_2 diffusivity

$\frac{D}{D_{EST}}$ [1]	Average[2] velocity	Gas hold-up	Conversion %
0,125	0,543	0,322	88,07
0,2	0,630	0,380	86,39
0,5	0,817	0,505	81,28
1,0	0,931	0,583	76,61
1,5	0,980	0,617	74,05

1. D_{EST} : CO_2 diffusivity as calculated in Appendix.
2. Average dimensionless superficial gas velocity.

5. MODEL EXTENSIONS

While this report was being written, a manuscript of a similar paper submitted for publication in "Chemical Engineering Science" by Stern et al.[26] was received. In this manuscript the PPF model is derived, including a fixed olefin to paraffin ratio in the product spectrum. The water-gas shift reaction is included either in the equilibrium form or through a finite rate expression. As a further improvement, axial dispersion in both the gas and liquid phases is included, giving a system of equations that is solved by collocation methods. In the axially dispersed case, the water-gas shift reaction has had to be incorporated in the form of a finite rate expression to permit solution of the model.

The model equations presented in the previous sections of this report can be changed to include the effect of olefin to paraffin ratio in the product spectrum. However, this was found not to alter the results predicted by this study markedly, except for providing more information about the water-gas shift reaction. If the fraction of alkanes in the products of carbon number 2 or higher is γ, the equations that test for the water-gas shift equilibrium change as shown:

The outlet gas velocity is now:

$$U_G = U_G^0(1 - YX_{CO+H_2})$$

where the molar contraction factor is:

$$Y = \frac{1 + \alpha + (1 - \alpha)^2 + \gamma\alpha(1 - \alpha)}{3 + (1 - \alpha)^2 + \gamma\alpha(1 - \alpha)} \tag{40}$$

Exit mole fractions for H_2, CO, H_2O, CO_2 and hydrocarbons of carbon number n become:

$$y_{H_2} = \frac{[1/(1 + 1)] - \sigma_{H_2} X_{CO+H_2} + t_2}{1 - YX_{CO+H_2}} \tag{41a}$$

$$y_{CO} = \frac{[1/(1 + 1)] - \sigma_{CO} X_{CO+H_2} - t_2}{1 - YX_{CO+H_2}} \tag{41b}$$

$$y_{H_2O} = \frac{\sigma_{H_2O} X_{CO+H_2} - t_2}{1 - YX_{CO+H_2}} \tag{41c}$$

$$y_{CO_2} = \frac{t_2}{1 - YX_{CO+H_2}} \tag{41d}$$

and

$$y_{C_n} = \frac{\sigma_{C_n} X_{CO+H_2}}{1 - YX_{CO+H_2}} \tag{41e}$$

The reaction stoichiometric coefficients are now:

$$\sigma_{H_2} = \frac{2 + (1 - \alpha)^2 + \gamma\alpha(1 - \alpha)}{3 + (1 - \alpha)^2 + \gamma\alpha(1 - \alpha)} \tag{42a}$$

$$\sigma_{CO} = \frac{1}{3 + (1 - \alpha)^2 + \gamma\alpha(1 - \alpha)} \tag{42b}$$

$$\sigma_{H_2O} = \frac{1}{3 + (1 - \alpha)^2 + \gamma\alpha(1 - \alpha)} \tag{42c}$$

and

$$\sigma_{C_n} = \frac{(1 - \alpha)^2 \alpha^{n-1}}{3 + (1 - \alpha)^2 + \gamma\alpha(1 - \alpha)} \tag{42d}$$

In the above equations t_2 is the number of CO_2 molecules formed per mole of synthesis gas entering the reactor. It is given by:

$$t_2 = \frac{B - \sqrt{B^2 - 4AC}}{2A} \tag{43a}$$

where

$$A = K_w - 1 \tag{43b}$$

$$B = \frac{K_w + 1}{1 + 1} - \sigma_{H_2} X_{H_2+CO} \tag{43c}$$

and

$$C = K_w q_{H_2O} \left(\frac{1}{1 + 1} - \sigma_{CO} X_{H_2+CO} \right) X_{H_2+CO} \tag{43d}$$

The H_2:CO usage ratio is

$$U = \frac{\sigma_{H_2} X_{CO+H_2} - t_2}{\sigma_{CO} X_{CO+H_2} + t_2} \tag{44}$$

Application of these equations to the data of Kuo et al.[22] shows that the water-gas shift reaction did not fully reach equilibrium in their reactor, as can be seen in Figure 13. The exit ratio is also seen to be fairly sensitive to the paraffin fraction γ of the C_2^+ products. If the fractional approach to water-gas shift equilibrium is estimated at 95 %, the data are well represented (Figure 13) by the theory. The fractional approach to water-gas shift equilibrium is defined as the ratio of the number of CO_2 molecules actually formed to the number required to be formed by the equilibrium condition. In the absence of kinetic data for the water-gas shift reaction, this reaction can therefore be taken to be in equilibrium without introducing a large error.

FIGURE 13 Effect of alkenes and fractional approach to WGS equilibrium

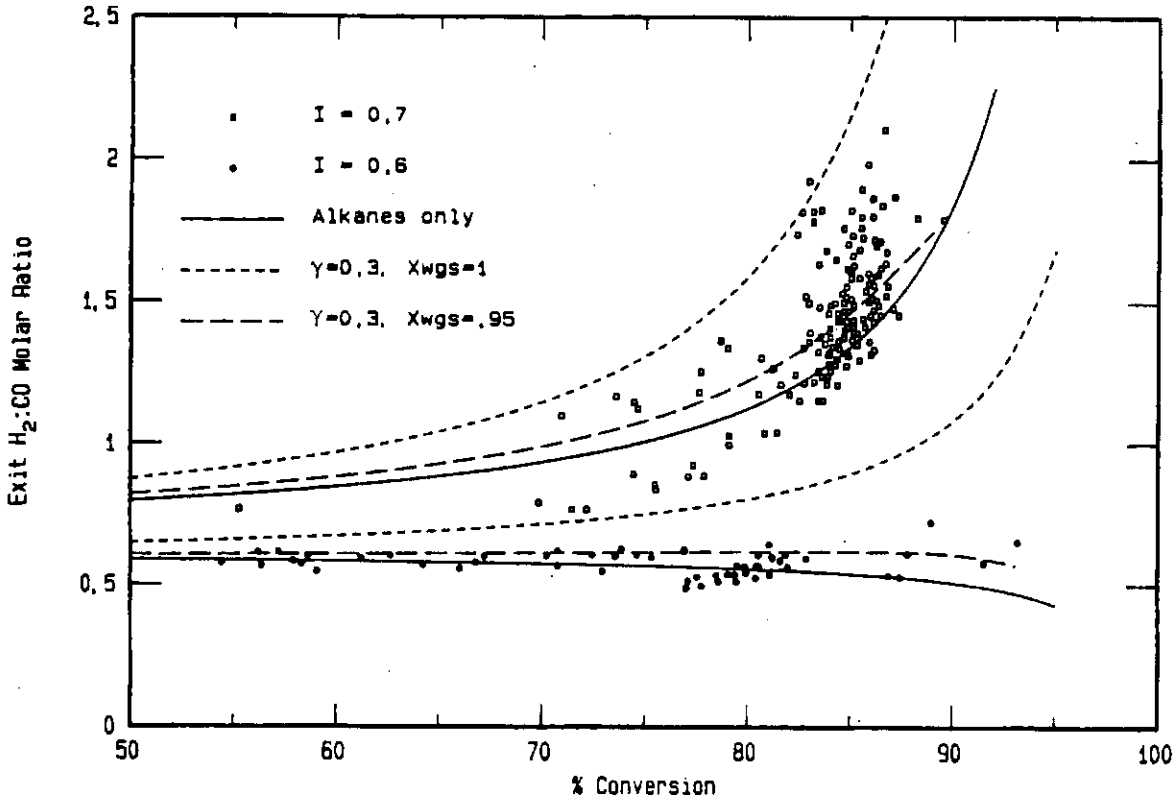

Effects and results found in this study which were overlooked by Stern et al.[26] are:

i. Evaluation of data in the relevant literature showed that the water-gas shift reaction can be assumed to be in equilibrium as a first approximation.

ii. An algebraic equation for the gas contraction factor is derived which is valid for the PPF model and also for the axially dispersed model of Stern et al.[26]; this point will be elaborated on in a follow-up paper.

iii. Algebraic solutions for the usage ratio and exit ratio are given, as well as an algebraic solution for the case of negligible mass transfer resistances.

iv. The hydrocarbons are found to approach gas-liquid equilibrium more rapidly as the carbon number increases. This makes lumping of the hydrocarbons as was done by Stern et al.[26] questionable.

v. The possibility of an initial increase in gas velocity in the reactor is pointed out for the first time, and in this regard the ratios of the Stanton numbers of the reactants and products under conditions of almost negligible mass transfer resistance are found to be important.

6. CONCLUSIONS AND RECOMMENDATIONS

i. The water-gas shift reaction approaches equilibrium in slurry reactors operating with iron-based catalysts at high conversions and temperatures above 523 K. In laboratory reactors emphasis must also be placed on the water-gas shift reaction to obtain a reliable reaction rate expression.

ii. F-T catalysts without a high activity for the water-gas shift reaction (e.g. ruthenium) must not be used in slurry reactors if benefit is to be derived from the lower cost of synthesis gas with a low H_2:CO ratio. High conversions, extensive back-mixing and catalysts that are active for the water-gas shift must be used when processing synthesis gas of low H_2:CO ratios at temperatures at which carbide formation may present problems.

iii. Heavy hydrocarbons can be assumed to be in equilibrium between the gas and liquid phases due to their high solubilities.

iv. Liquid back-mixing reduces conversion but increases catalyst life. The best degree of back-mixing from an economic point of view is not necessarily perfect mixing or zero mixing. Means of controlling back-mixing should be investigated.

v. In large slurry reactors operating at high gas velocities the mass transfer rates are high relative to reaction kinetics, but the ratios of mass transfer rates of reactants and products influence the gas velocity profiles in the reactors significantly. This in turn affects the gas hold-up and the reactor space available for the catalyst and hence the overall reactor performance. Gas hold-ups, mass transfer rates and reaction kinetics (particularly in the case of catalysts with relatively high activity) will have to be measured accurately before slurry reactors can be scaled-up reliably.

7. REFERENCES

1. KOLBEL, H and RALEK, M. The Fischer-Tropsch synthesis in the liquid phase. *Catal. Rev. Sci. Eng.*, 21 (2), 1980, p 225.

2. FUJIMOTO, K and KUNUGI, T. Review of slurry phase Fischer-Tropsch synthesis. *Proc. PAN-PAC Synfuels Conf.*, 1, 1982, p 167.

3. CALDERBANK, P H, EVANS, F, FARLEY, R, JEPSON, G and POLL, A. *Rate processes in the catalyst-slurry Fischer-Tropsch reaction.* Proc. Symp. Catalysis in Practice, Instn. Chem. Engrs, 1963, p 66.

4. SATTERFIELD, C N and HUFF, G A. Effect of mass transfer on Fischer-Tropsch synthesis in slurry reactors. *Chem. Eng. Sci.*, 35, 1980, p 195.

5. SCHLESINGER, M D, BENSON, H E, MURPHY, E M and STORCH, H H. Chemicals from the Fischer-Tropsch synthesis. *Ind. Eng. Chem.*, 46 (6), 1954, p 1322.

6. DECKWER, W-D, SERPEMEN, Y, RALEK, M and SCHMIDT, B. On the relevance of mass transfer limitations in the Fischer-Tropsch slurry process. *Chem. Eng. Sci.*, 36, 1981, p 765.

7. QUICKER, G and DECKWER, W-D. Gas hold-up and interfacial area in aerated hydrocarbons. *Ger. Chem. Eng.*, 4, 1981, p 363.

8. BUKUR, D B. Some comments on models for Fischer-Tropsch reaction in slurry bubble column reactors. *Chem. Eng. Sci.*, 38, (3), 1983, p 441.

9. VAN VUUREN D S. Mass transfer limitations in Fischer-Tropsch slurry reactors. *Chem. Eng. Sci.*, 38, 1983, p 1365.

10. DECKWER, W-D, SERPEMEN, Y, RALEK, M and SCHMIDT, B. Modelling the Fischer-Tropsch synthesis in the slurry phase. *Ind. Eng. Chem. Process Des. Dev.*, 21 (2), 1982, p 231.

11. STERN, D, BELL, A T and HEINEMANN, H. Effects of mass transfer on the performance of slurry reactors used for Fischer-Tropsch synthesis. *Chem. Eng. Sci.*, 38, 1983, p 597.

12. SATTERFIELD, C N and HUFF, G A. Usefulness of a slurry type Fischer-Tropsch reactor for processing synthesis gas of low hydrogen to carbon monoxide ratios. *Can. J. Chem. Eng.*, 60, 1982, p 159.

13. SATTERFIELD, C N and HUFF, G A. *Intrinsic kinetics of the Fischer-Tropsch synthesis on a reduced fused-magnetite catalyst.* Paper presented at the AIChE Annual Meeting, Los Angeles, Paper 120e, 1982.

14. DECKWER, W-D, LEDAKOWICZ, S and SANDERS, E. Studies on the Fischer-Tropsch synthesis in slurry phase. *Proc. AIChE meeting,* Philadelphia, Paper 14d, 1984.

15. CALDWELL, L, and VAN VUUREN, D S. *On the formation and composition of the liquid phase in Fischer-Tropsch reactors.* Chem. Eng. Sci. (in press).

16. FINLAYSON, B A. *Nonlinear analysis in chemical engineering.* McGraw-Hill , 1980.

17. DRY M E, SHINGLES, T and BOSHOFF, L J. Rate of the Fischer-Tropsch reaction over iron catalysts. *J. Catalysis*, 25, 1972, p 99.

18. FARLEY, R and RAY, D J. The design and operation of a pilot scale plant for hydrocarbon synthesis in the slurry phase. *J. Inst. Petroleum*, 50 (482), 1964, p 27.

19. CALDWELL, L. *Selectivity in Fischer-Tropsch synthesis: review and recommendations.* CSIR Report CENG 330, 1980.

20. SCHLESINGER, M D, CROWELL, J H, LEVA, M and STORCH, H H. Fischer-Tropsch synthesis in slurry phase. *Ind. Eng. Chem.*, 43 (6), 1951, p 1474.

21. KOPPERS, H H. Rheinpreussen-Koppers liquid-phase process of Fischer-Tropsch synthesis. *Chemical Age of India*, 12, 1961, p 7.

22. KUO, J C W, LIEB, T M, GUPTE, K M and KYAN, C P. Two-stage slurry Fischer-Tropsch/ZSM-5 process. *Proc. AIChE Spring National Meeting*, Anaheim, 1984.

23. Hugo W J. *The Fischer-Tropsch reaction in a three-phase reactor*. M.Sc. Thesis, Potchefstroom University for CHE, 1984.

24. LEITH, I R. Private communication, 1985.

25. DECKWER, W-D, LOUISI, Y, ZAIDI, A and RALEK, M. Hydrodynamic properties of the Fischer-Tropsch slurry process. *Ind. Eng. Chem. Process Des. Dev.*, 19 (4), 1980, p 699.

26. STERN, D, BELL, A T and HEINEMANN, H. *A theoretical model for the performance of bubble column reactors used for Fischer-Tropsch synthesis.* Paper submitted for publication in Chem. Eng. Sci.

27. PETER, S and WEINERT, M. Uber die Löslichkeit von H_2, CO, CO_2 und Wasserdampf in flüssigen Kohlenwasserstoffen. *Z. Phys. Chem.*, 5, 1955, p 114.

28. SAGE, B H, BACKUS, H S and LACEY, W N. Phase equilibria in hydrocarbon systems. VIII Methane-crystal oil system. *Ind. Eng. Chem.*, 27 (6), 1935, p 686.

29. CALDERBANK, P H and MOO-YOUNG, M B. The continous phase heat and mass transfer properties of dispersions. *Chem. Eng. Sci.*, 16, 1961, p 39.

30. REID, R C, PRAUNITZ, J M and SHERWOOD, T K. *The properties of gases and liquids.* (Third edition), McGraw-Hill , 1977.

8. APPENDIX : PARAMETER ESTIMATION

8.1 Reaction rate parameters

The parameters k_{FT} and b in Equation (10) are obviously strong functions of the catalyst used. Values obtained for the catalyst used by Satterfield and Huff[19] are:

$$k_{FT} = 3940\exp\left(\frac{-9910}{T}\right) \text{mol kg}^{-1}_{\text{catalyst}}\, s^{-1}\, kPa^{-1} \quad (A1)$$

$$b = 1{,}0 \times 10^{7} \exp\left(\frac{-12100}{T}\right) kPa^{-1} \quad (A2)$$

Parameter k_{FT} (the catalyst activity) was varied arbitrarily in the calculations, whereas in all cases parameter b was estimated by using Equation (A2).

8.2 Fluid dynamic properties

The experimental results of Deckwer et al.[25] are considered to be the most reliable in the literature. They recommend the following:

$$\epsilon = 8{,}4(U_G^0)^{1{,}1} \quad (A3)$$

$$d = 7 \times 10^{-4}\ m \quad (A4)$$

$$a = 6\epsilon/d\ m^{-1} \quad (A5)$$

However, the correlation for the gas hold-up and the bubble diameter was derived from data obtained from laboratory experiments with bubble columns operating at superficial gas velocities of less than 0,04 m s^{-1}, which is well below the velocity of 0,095 m s^{-1} specified for the Rheinpreussen-Koppers slurry reactor. The correlation can therefore not be used with confidence at such high velocities even though a data point at 0,073 m s^{-1} reported by Farley and Ray[18] corresponds with the correlation (Deckwer et al.[25]). Deckwer et al.[10] also presented data of Hammer (1968) showing that the gas hold-up increases with increasing velocity up to a value of about 0,45, after which it remains constant. It was therefore decided to use a value of 0,45 for the gas hold-up in the numerical examples. In the example in which the effect of the ratios of the mass transfer rates is considered, the gas hold-up was varied according to Equation (A3) and for the velocity term, the average velocity in the reactor was used.

8.3 Gas solubilities

Very little data are available on the solubilities of the various gases in F-T reactor wax. For the purpose of this report, the data reported by Peter and Weinert[27] for the solubilities of hydrogen, carbon monoxide, carbon dioxide and water in paraffin wax were used. When a straight-line correlation for the wax density (data by Calderbank et al.[8]) and the ideal gas law are used, the data of Peter and Weinert can be transformed to the following equations:

$$m_{H_2} = \frac{4{,}02 \times 10^5 \exp[740{,}3/T]}{(1008 - 0{,}6018T)T} \qquad \text{(A6a)}$$

$$m_{CO} = \frac{4{,}99 \times 10^5 \exp[458{,}3/T]}{(1008 - 0{,}6018T)T} \qquad \text{(A6b)}$$

$$m_{CO_2} = \frac{1{,}23 \times 10^6 \exp[-373/T]}{(1008 - 0{,}6018T)T} \qquad \text{(A6c)}$$

$$m_{H_2O} = \frac{4{,}05 \times 10^6 \exp[-1229/T]}{(1008 - 0{,}6018T)T} \qquad \text{(A6d)}$$

Apart from the solubility of methane in crystal oil (Sage et al.[28]), to the author's knowledge no data are available in the open literature on the solubilities of light alkanes in liquids similar to wax at synthesis conditions. Approximate values can be calculated by using Raoult's law and the ideal gas law, viz.

$$m_{C_n} = \frac{P^o_{C_n}}{RTC_L} \qquad \text{(A7)}$$

Approximate values of the pure component vapour pressures are (Caldwell and Van Vuuren[15])

$$P^o_{C_n} = 1{,}78382 \times 10^6 \exp\left(-427{,}218\left(\frac{1}{T} - 1{,}029807 \times 10^{-3}\right) n\right) \text{kPa} \qquad \text{(A8)}$$

We assume that the average hydrocarbon chain length of Krupp wax is 24. This was the average chain length of the wax used by Peter and Weinert[27] and it also falls within the range of average chain lengths for normal synthesis conditions as calculated by Caldwell and Van Vuuren[15]. At that average chain length the molar density is approximately:

$$C_L = 3000 - 1,79T \text{ mol m}^{-3} \quad (A9)$$

At 543 K the calculated solubility coefficients of methane and pentane are then 1,38 and 0,4 respectively. This solubility coefficient of methane agrees remarkably well with the value estimated by Stern et al.[11], and the value for pentane is lower than the value for methane as it is expected to be, and not higher as estimated by Stern et al.[11].

8.4 Liquid flow rate

The liquid flow rate may be an independent process variable if wax is recirculated to the reactor. It is, however, more likely for the reactor to operate with a batch of wax, in which case only a small stream of excess wax produced by the synthesis will be withdrawn. The liquid flow rate can then be ignored or, alternatively, it can be estimated by the method used by Caldwell and Van Vuuren[15].

8.5 Mass transfer coefficients

To estimate the mass transfer coefficients for small bubbles (less than about 2,5 to 3 mm), the well-known correlation of Calderbank and Moo-Young[29] can be reduced to

$$k_{L,i} = 0,31\left(\frac{D_{L,i}^2 \rho_L g}{\mu_L}\right)^{1/3} \quad (A10)$$

Satterfield and Huff[4] estimated the hydrogen diffusivity to be:

$$D_{L,H_2} = 7,35 \times 10^{-7}\exp(-2285/T) \quad (A11)$$

The diffusivities of the other compounds can be derived from the hydrogen diffusivity using the Wilke-Chang correlation (Reid et al.[30]), viz.

$$D_{L,i} = D_{L,H_2}(v_{H_2} / v_i)^{0,6} \quad (A12)$$

For diffusivity calculations a molar volume of $14,3 \times 10^{-6}$ m^3 mol^{-1} for hydrogen is normally used. The molar volumes of the other components can be calculated by the Schroeder method (Reid et al.[30]), viz.

$$v_{CO} = 30,7 \times 10^{-6} \text{ m}^3 \text{ mol}^{-1}$$

$$v_{CO_2} = 34,0 \times 10^{-6} \text{ m}^3 \text{ mol}^{-1}$$

$$v_{H_2O} = 18,9 \times 10^{-6} \text{ m}^3 \text{ mol}^{-1}$$

$$v_{C_n} = 7(3n + 2) \times 10^{-6} \text{ m}^3 \text{ mol}^{-1}$$

The density and viscosity data of Calderbank et al.[9] can be represented respectively by:

$$\rho_L = 1008 - 0,6018T \qquad (A13)$$

and

$$\mu_L = ((1,64 \times 10^{-5}) \exp(2482/T) \qquad (A14)$$

8.6 Water-gas shift equilibrium coefficient

This has been given by Satterfield and Huff[12] as

$$K_w = 0,0102 \exp(4730/T) \qquad (A15)$$

9. NOMENCLATURE

A	coefficient in Equation (39a)	
a	gas-liquid interfacial area per unit reactor volume	m^{-1}
B	coefficient in Equation (39a)	
b	parameter in rate expression	kPa^{-1}
C	coefficient in Equation (39a)	
C_G	gas-phase molar concentration	$mol\ m^{-3}$
$C_{G,i}$	gas-phase concentration of component i	$mol\ m^{-3}$
$C^o_{G,i}$	gas-phase concentration of component i at inlet	$mol\ m^{-3}$
$\bar{C}_{G,i}$	average gas-phase concentration of component i	$mol\ m^{-3}$
C_L	liquid-phase molar concentration	$mol\ m^{-3}$
$C_{L,i}$	liquid-phase concentration of component i	$mol\ m^{-3}$
$D_{L,i}$	liquid-phase diffusion coefficient of component i	$m^2\ s^{-1}$
d	average bubble diameter	m
E	error caused by neglecting hydrocarbon components with carbon number higher than specified	
g	gravitational acceleration	$m\ s^{-2}$
I	inlet H_2:CO molar ratio	
i	component i	
K_w	water-gas shift equilibrium coefficient	
k_{FT}	catalyst activity or reaction rate constant	$mol\ kg^{-1}\ kPa^{-1}$
$k_{L,i}$	gas-liquid interfacial mass transfer coefficient	$m\ s^{-1}$
L	reactor length	m

m_i	solubility coefficient of component i	
N_i	Stanton number of component i	
n	carbon number	
n_1	reaction rate of CO via F-T reaction and F-T synthesis gas consumption rate	
n_2	ratio of consumption rate of CO via water-gas shift reaction and F-T synthesis gas consumption rate	
$P^0_{C_n}$	pure component vapour pressure of hydrocarbon of carbon number n	kPa
p_i	partial pressure of component i	
Q_L	liquid volumetric flow rate leaving the reactor	$m^3 s^{-1}$
R	gas constant	
r_i	consumption rate of component i	$mol\ kg^{-1} s^{-1}$
r_{H_2+CO}	synthesis gas consumption rate	$mol\ kg^{-1} s^{-1}$
T	temperature	K
t_1	moles of CO converted via F-T reaction per mole of synthesis gas fed to reactor	
t_2	moles of CO_2 produced per mol of synthesis gas fed to reactor	
U	H_2:CO usage ratio	
U_G	superficial gas velocity	$m\ s^{-1}$
U^0_G	superficial gas velocity at reactor inlet	$m\ s^{-1}$
V	reactor volume	m^3
v_i	molar volume of component i	$m^3\ mol^{-1}$

w	catalyst concentration	$kg\ m^{-3}$
X_{CO+H_2}	fractional conversion of synthesis gas	
Y	molar contraction factor	
y_i	fractional gas phase concentration of component i	
z	reactor co-ordinate	m

Greek letters

α	chain-growth probability	
α_m	chain-growth probability at maximum error	
γ	paraffin fraction of C_2^+ products	
ε	gas hold-up	
ζ	dimensionless reactor co-ordinate	
θ_G	dimensionless gas molar contraction	
$\theta_{G,i}$	dimensionless gas phase concentration of component i	
$\bar{\theta}_{G,i}$	average dimensionless gas phase concentration of component i	
$\theta_{l.,i}$	dimensionless liquid phase concentration of component i	
μ_L	liquid viscosity	$kg\ m^{-1}\ s^{-1}$
ν	dimensionless superficial gas velocity	
ρ_L	liquid density	$kg\ m^{-3}$
σ_i	stoichiometric coefficient of component i	
ω_G	gas space velocity	s^{-1}
ω_L	liquid space velocity	s^{-1}